European Cooperation in Science and Technology (COST) is a funding organization for the creation of research networks, called COST Actions.

EsSENce Cost Action CA19118

Project Title:

"High-performance Carbon-based composites with Smart properties for Advanced Sensing Applications"

Deliverable No	D3.1
Deliverable Title	Guidelines and Codes of good practices referring to the manufacturing processes of CNM composites
Working Group	3
Originator	INEGI

cost EUROPEAN COOPERATION IN SCIENCE & TECHNOLOGY

Funded by the Horizon 2020 Framework Programme of the European Union

DISCLAIMER

This document contains the description of the COST Action EsSENce CA19118 project findings, work and products. Certain parts of it might be under partner Intellectual Property Right (IPR) rules. Therefore, prior to using its content please contact the consortium coordinator for approval. E-mail: charitidis@chemeng.ntua.gr .

Should you feel that this document harms in any way the IPR held by you as a person or as a representative of an entity, please do notify us immediately.

The authors of this document have taken all available measures in order for its content to be accurate, consistent and lawful. However, neither the project consortium as a whole nor the individual partners that implicitly or explicitly participated in the creation and publication of this document hold any sort of responsibility that might occur as a result of using its content.

This document has been produced with the assistance of the European Union. The content of this document is the sole responsibility of the EsSENce consortium and can in no way be taken to reflect the views of the European Union.

Table of Contents

1 Project Summary....5
2 Carbon-based nanomaterials....6
2.1 Fullerenes....6
2.2 Carbon nanodots....7
2.3 Carbon nanotubes....8
2.4 Carbon nanofibers....9
2.5 Graphite....9
2.6 Graphene....10
2.7 Graphene oxide (GO)....13
2.8 Reduced graphene oxide (rGO)....15
2.9 Graphene nanoribbons....16
2.10 Graphene-like materials....16
2.11 Bio-based CNM....17
3 Thermoset-based composites....21
3.1 Difficulties to disperse CNM in thermoset matrices....21
3.2 Strategies to maximize properties of CNM in thermoset nanocomposites....21
3.2.1 Ultrasonication....22
3.2.2 Calendering....23
3.2.3 Functionalization....24
3.3 Carbon fibre reinforced polymer composites....26
3.3.1 Matrix modification....27
3.3.2 Fibre modification....29
4 Thermoplastic-based composites....30
4.1 Main drawbacks when using CNM in thermoplastics....31
4.2 Strategies to maximize the properties of the CNM based composites....31
4.2.1 Enhancing interfacial interactions between CNM and thermoplastics....31
4.2.2 Enhancing dispersion of CNM in thermoplastics....32
4.2.3 Adapting the CNM content to find the optimum for the desired application....33
5 Other applications of CNM....35
5.1 Metal Organic Framework composites....35
5.2 Coatings prepared by Matrix Assisted Pulsed Laser Evaporation technique....37
6 Conclusion....39
7 References....40

Table of Figures

Figure 1 Different types of carbon-based nanomaterials. 6

Figure 2 Graphene oxide structure [96]. 13

Figure 3 Comparison among the main chemical protocols to produce GO. 14

Figure 4 Main approaches to manufacture modified CFRP with CNM. 27

Figure 5 Illustration of the reinforcement from the modified fibres with CNT in the hybrid composites. 29

Table of Tables

Table 1 List of graphene's main properties. 11

Table 2 Summary of the methods used for graphene preparation [79, 82, 83]. 11

Table 3 Recent studies on bio-based carbon materials. 18

Table 4 Resume of advantages and disadvantages of each dispersion methods [181, 182, 209]. 26

List of abbreviations

0D	Zero-dimensional
1D	One-dimensional
2D	Two-dimensional
AFM	Atomic force microscopy
Bio-CNTC	Bio-oil based carbon nanotubes cotton
CB	Carbon black
CDs	Carbon nanodots
CF	Carbon fibre
CFRP	Carbon fibre reinforced polymer
CNF	Carbon nanofibers
CNM	Carbon nanomaterials
CNT	Carbon nanotubes
CPC	Conductive polymer composites
CVD	Chemical vapor deposition

EMI	Electromagnetic interference
FCCVD	Floating catalyst chemical vapor deposition
FESEM	Field Emission Scanning Electron Microscopy
GIC	Graphite intercalation compounds
GL	Graphene-like layers
GLox	Graphene-like layers oxidized
GNR	Graphene nanoribbons
GO	Graphene oxide
GRM	Graphene related materials
HOPG	Highly oriented pyrolytic graphite
MAPLE	Matrix Assisted Pulsed Laser Evaporation
MOF	Metal organic frameworks
MOFs	Metal organic frameworks
MWCNT	Multi-walled carbon nanotubes
PA12	Polyamide 12
PE	Polyethylene
PEG	Polyethylene glycol
PP	Polypropylene
PL	Photoluminescence
PSO	Particle swarm optimisation
rGO	Reduced graphene oxide
SEM	Scanning electron microscopy
SiC	Silicon carbide
SWCNT	Single-walled carbon nanotubes
TRL	Technology readiness level
UD	Unidirectional

1 Project Summary

The goal of EsSENce Cost Action is to develop a scientific & technological innovation hub at European and International level, focusing on advanced composite materials reinforced with carbon-based nanomaterials for sensing applications.

The main focus of the scientific community is to combine advances in manufacturing technologies with the development of innovative nano-enabled composite materials for the fabrication of lightweight smart devices with structural performance and improved and/or added new functionalities including sensing and detection.

The advent of sensors in many different applications, including environmental monitoring, monitoring constituents in food products, security, gas sensing as well as diagnostics and human health monitoring, has led to the ever-growing modification of existing processing and manufacturing routes by incorporating advanced carbon-based reinforced composites, which are able to offer multifunctionalities. Among the applications of carbon based (nano)material composites, lightweight and smart sensors, which will provide highly accurate and real-time monitoring functions in different equipment and devices without the cost of structural integration, is the area that is particularly focused on EsSENce.

The deliverable 3.1 (D3.1) entitled Guidelines and Codes of good practices referring to the manufacturing processes of carbon nanomaterials (CNM) composites, was developed within the WG3 regarding novel CNM & new processing routes. At first, a brief overview of the different carbon-based nanomaterials with potential utilization in sensing applications is presented. Followed by the different methodologies used to prepare nanocomposites and fibre reinforced composites, along with their main properties. The main purpose of this document is to give a clear view of the drawbacks that limit the up-scale utilization of CNM composites and to provide principles and strategies for the maximization of their properties with the incorporation of these types of particles. This deliverable received contribution from the following WG3 members: Andreia Araujo, Ayfer D. Cavdar, Beate Krause, Dejan Kepic, Michela Alfe, Petra Pötschke, Raquel M. Santos and Valentina Gargiulo.

2 Carbon-based nanomaterials

In the past several decades, it was observed an emergence in the nanotechnology field, that has stimulated a wide range of researches in various fields and disciplines to evolve from theory to practical applications. In particular, carbon, the basic element for life on Earth, has been attracted a great deal of attention, owing to its ability to form different types of hybridization states (*sp, sp*^{2} and *sp*^{3}) that makes it capable of forming a wide range of allotropes. In this sense, carbon nanomaterials (CNM), with their tunable physical, chemical and electrical properties (among others), have been extensively studied and have inspired innovative solutions to current environmental, health and engineering challenges [1, 2]. According to their spatial dimensions, CNM can be roughly divided into zero-dimensional (0D), as for example fullerenes, one-dimensional (1D), such as single-walled or multi-walled carbon nanotubes (CNT, SWCNT, MWCNT) and carbon nanofibers (CNF), or two-dimensional (2D), particles from the graphene family like graphene sheets and few layers graphene (Figure 1) [3].

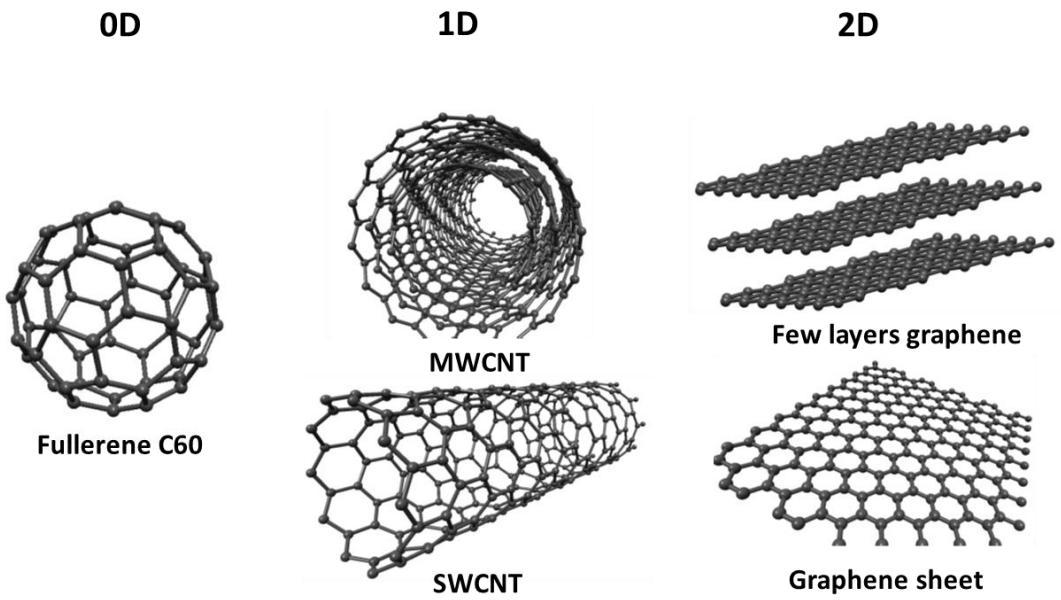

Figure 1 Different types of carbon-based nanomaterials.

2.1 Fullerenes

Fullerenes are a family of hollow spherical or ellipsoid molecules that consist of carbon atoms arranged in pentagons and hexagons. The representative of this family is molecule C_{60}, also known as buckminsterfullerene named after architect Buckminster Fuller, composed of 12 pentagons and 20 hexagons in a closed cage of 60 carbon atoms [4]. The C_{60} molecule has the van der Waals diameter of 1.1 nm [5]. Generally, fullerenes are 0D materials described by the notation C_{2n}, where n is an integer higher or equal to 10, with C_{20} or dodecahedral being the smallest stable fullerene. Although carbon in fullerene molecules is *sp*^{2} hybridized, the curvature of molecules causes an unequal extension of *p* lobes at the outer and inner surface of the sphere giving rise to the p character, therefore carbon atoms in fullerenes have a pseudo *sp*^{3} character [6]. While the curvature increases the electron affinity of carbon atoms, which is reflected in the increased reactivity, with the increase in the number of carbon atoms, the electron affinity and reactivity decrease due to the weakening of the curvature effect [7]. Although fullerenes are chemically stable, the angle strain causes electrophilic addition reactions. Moreover, some carbon atoms from the cage can be substituted with a heteroatom, such as nitrogen, oxygen,

boron, etc. to create heterofullerenes [8-10]. In fact, atoms or clusters of atoms can be encapsulated in fullerenes to form endohedral fullerenes [11].

Fullerenes can be found in nature either as aggregates or in the form of crystal structures [12]. They can be also synthesized by employing different methods, namely laser ablation or arc discharge from graphite as a source material [13, 14], or *via* the combustion of hydrocarbons [15]. The aforementioned processes result in a mixture of fullerenes and some other forms of carbon, and therefore, require an additional purification step. Usually, fullerenes are extracted using a certain solvent (these particles are soluble in organic solvents such as 1-chloronaphthalene, carbon bisulfide, toluene, and chlorobenzene [16]) and then separated employing chromatography such as liquid chromatography or supercritical fluid chromatography. To date, the purification and separation step still represents a challenge and one of the key factors that determine the fullerene price.

Due to their electrical and photophysical properties, fullerenes were investigated for sensing applications [17]. Fullerenes' ability to accept electrons can be used for the immobilization of fullerene molecules with different enzymes which further leads to the development of a sensor for glucose [18, 19] or urea [20]. Besides, fullerenes and fullerene-based hybrids were studied also for gas sensing [21, 22], electrochemical sensing [23, 24], and optical sensing [25].

2.2 Carbon nanodots

Carbon nanodots (CDs) were accidentally discovered by Xu et al. [26] in 2004 while using preparative electrophoresis to purify the SWCNT synthesized from soot by arc-discharge method. Unique properties, simplicity of synthesis procedures and diversity of initial raw-materials along with tunable photoluminescence (PL) behaviour through surface passivation of CNM, make them a promising candidate for a wide range of applications. Another key element that fuels interest in CDs is that they can be produced on a large scale (frequently using a one-step pathway and potentially from biomass waste-derived sources) by many approaches, gatherable as top-down and bottom-up methods. Top-down approaches include: arc discharge, laser ablation and acidic oxidation of bulk carbon-based materials, and electrochemical synthesis. Bottom up approaches include: combustion processes (including simple candle burning), pyrolysis (also microwave assisted) of sugars and simple carbon rich molecules, hydrothermal synthesis, and chemical vapor deposition [27-30]. Although CDs synthesis is cheap and robust, it may require complex procedures of separation and purification to ensure an effective extraction of the material of interest. The common view currently considers the CDs as quasi-spherical nanoparticles comprising a highly defected composition of coexisting aromatic (sp^2 hybridized two-dimensional graphene-type islands) and aliphatic (sp^3 hybridized diamond-type inclusions) regions that are assembled in proportions and with variations of surface groups that depend on the conditions of their synthesis [31]. Polar groups derived from starting materials in the formation of nanoparticles are found at the surface, allowing the particles to be well-dispersed in water. Typically, CDs of different origins contain high amounts of carboxylic groups, and also, some hydroxyls and carbonyls at their surface, imparting them with excellent water solubility and the suitability for subsequent functionalization with other organic, polymeric, inorganic, or biological species [32].

CDs exhibit many fascinating optical properties, such as size- and wavelength-dependent photoluminescence (PL), photoinduced electron transfer, up-conversion luminescence, chemiluminescence and electrochemiluminescence [27, 33]. All these advances make CDs a promising material for a new generation of fluorophore biosensors, biomedical imaging [34, 35], drug delivery development for applications in bioscience and nanobiotechnology [32, 36, 37], composite materials preparation [38] and optoelectronic devices development [39].

Many studies on various types of cell lines, at different concentrations, and with or without surface coverages have demonstrated that CDs exhibit very low toxicity and can be easily internalized into cells for imaging. In almost all of cases, CDs have been demonstrated to cause negligible loss in cell viability, even after a long period of exposure at high concentrations [40, 41]. In particular, Havrdova et *al.* [40] found that CDs toxicity is strictly related to their surface charge (negative, neutral or positive): functionalized CDs with polymers (polyethylene glycol, PEG) determining a neutral surface charge would be an appropriate method for *in vivo* imaging, while CDs stabilized with negatively charged carboxylate groups can induce abnormalities in the cell cycle at higher concentrations. CDs imaging for the on-gels detection of human serum proteins and Escherichia coli proteins after polyacrylamide gel electrophoresis showed that the sensitivity of CDs imaging is 8 times higher than the sensitivity of traditional Coomassie brilliant blue-R250 staining [42]. For analytical purposes CDs have already been used as a luminescent label for protein detection (thrombin) [43], for the detection of sewage water bacteria [44], for biosensing of physiological pH (in a range between pH 6.0-7.5) in living cells as well as tissues at depths of 65-185 μm [45] and also, as nanosensors for metal ions detection [46].

2.3 Carbon nanotubes

Carbon nanotubes (CNT) are cylindrical hollow structures composed of one or more layers of rolled-up graphene [47, 48]. Depending on the number of consisting graphene layers, CNT can be single-walled (SWCNT) composed of a single graphene layer or multi-walled carbon nanotubes (MWCNT) which consist of several concentrically arranged layers with an interlayer distance of approximately 0.33 nm. The outer diameter of MWCNT usually lies between 3-15 nm, while SWCNT are narrower and have diameters in the 0.7-2 nm range [49]. With lengths that could be up to tens of micrometres and diameter on a nanometre scale, CNTs are considered nearly one-dimensional (1D) entities. CNT are lightweight because they are composed of only carbon while the covalent sp^2 carbon-carbon bonds contribute to their strength. Their Young's modulus range from 270-950 GPa and tensile strength 11-63 GPa [50] which could be used for ultra-high performance materials. MWCNT show ballistic conductor behaviour at room temperature [51]. However, depending on how the graphene sheet is rolled, i.e. the angle between hexagons and tubular axis, CNT can be either chiral or achiral. The chiral nanotubes possess a screw symmetry and achiral nanotubes have cylindrical symmetry. If the two hexagonal edges of achiral tubes are parallel to the axis of the cylinder the nanotube is considered zig-zag. On the other hand, if the two edges of a hexagon of achiral tubes are perpendicular to the axis of the cylinder the nanotube is an armchair. The angle between hexagons and tubular axis also determines whether the nanotube has metallic or semiconducting behaviour. This effect occurs due to the symmetry break of the planar system, which imposes a distinct direction with respect to the hexagonal lattice and the axial direction [52]. The bandgap of semiconducting nanotubes is diameter dependent and ranges from 0.1 to 0.2 eV [53].

CNT are produced using arc-discharge method, laser ablation, or chemical vapor deposition (CVD) technique [54]. To date, a preferential synthesis of metallic or semiconducting SWCNTs with a selectivity of 90-95 % has been achieved, however, the production of purely semiconducting SWCNTs is cost-prohibitive [55]. Precise control over CNT' diameter and chirality still represents a challenge. A particular challenge is to obtain CNT that are defect-free. Present separation techniques are not suitable for large-scale production. Also, produced CNT require the purification step to remove carbonaceous impurities and catalyst nanoparticles, which makes the overall process costly [54].

It has been found that the electrical properties of CNT are sensitive to doping by certain molecules [56, 57]. Besides, strain and bending of SWCNT could induce changes in their conductance [58]. These properties pave the way for CNT to be applied for sensing. Their high surface area and high adsorption capacity have been used to develop several types of gas sensors, such as sorption sensors, ionization

sensors, capacitance sensors, and resonance frequency shift gas sensors [53]. The occurrence of oxidation and reduction reactions during the interaction of CNT with biomolecules led to the development of CNT-based electrochemical sensors for biomedical applications [59]. Although the sidewalls of CNT are generally considered non-reactive, they could be functionalized covalently or non-covalently with various molecules or functional groups [60]. The functionalization provides additional opportunities for sensing applications of CNT by improving their selectivity and sensitivity [61].

Moreover, intrinsically conductive networks formed through the incorporation of CNT into polymeric matrices have been extensively investigated as a promising route for detecting, evaluating and monitoring the health of structural components in highly demanding sectors, including aeronautics and renewable energy. The strain sensing applications of modified polymer matrices with CNT are based on piezoresistivity, i.e. the electrical resistance variation when stress/strain stimuli are applied, induced by the change of connections between conductive fillers in the polymeric matrix. For those applications, the successfully preparation of nanocomposites with high electrical conductivity, at ultralow contents of CNT, is crucial since it allows the prevention of elasticity loss and the retention of other important properties as sensing sensitivity.

2.4 Carbon nanofibers

For the first years after its discovery, the occurrence of carbon nanofibers (CNF), often referred to as carbon filaments or filamentous carbon, was considered a nuisance. The fibres frequently occurred in metallic catalysts used for the conversion of carbon-containing gases. CNF possess filament structures based on sp^2 carbon arranged in conical or cylindrical shapes. Similar to CNT, CNF are considered 1D nanostructures due to their high length-to-diameter ratio. Their diameters typically are in the range of 3-100 nm, while the lengths are up to several hundreds of micrometres. They have high mechanical strength, flexibility, thermal stability, and porosity, but they also have more defects compared to CNT [62].

CNFs can be synthesised via CVD or electrospinning [63, 64]. The quality of the prepared CNFs is greatly influenced by the shape and size of metallic catalyst nanoparticles in the CVD and the polymer type in the electrospinning method. For instance, vertically aligned CNFs have been fabricated with help of Cu-Ni composition, while amorphous CNFs have been synthesized by ion beam irradiation [65].

Alike other CNM, CNFs have a large surface area. When applied as an electrode, CNF can greatly enhance the surface area of the electrode materials which improves the chemical interaction between electrode and analyte and increase the sensitivity. This combined with CNF' electrocatalytic ability to oxidize certain organic compounds makes them suitable for the detection of specific molecules, proteins, and nucleic acids [66, 67], and also for biomedical applications including wound dressing and bone tissue engineering [68]. Their chemical inertness and high mechanical strength provide long-term sensor stability. For various sensing applications, CNFs can be used as pristine or loaded with metallic nanoparticles, metal oxides, etc [69]. Similar to CNT, the incorporation of CNF into polymeric matrices allow the production of nanocomposites having self-sensing abilities.

2.5 Graphite

Graphite occurs naturally as a black lustrous mineral and it is mined in many places worldwide. Natural graphite exists in three different forms (graphite flakes, amorphous graphite and crystalline graphite) and often contains metal impurities, which type and amount vary on the basis of the extraction site [70]. Along these natural forms, two other forms of graphite are reported, namely kish graphite and synthetic graphite [70, 71]. Kish graphite is obtained as a by-product of the steel-making process and

contains residual iron impurities [71]. Synthetic graphite is obtained through high temperature processes (mostly pyrolysis processes) [72], its highly pure and ordered, also widely known as highly oriented pyrolytic graphite (HOPG) [73]. Owing to its excellent physical properties and low level of impurities, HOPG is used as scanning electron microscopy (SEM) support and length standard, as reference for most spectroscopies and is the starting material for the production of high quality and high pure graphene for utilization in electronics, magnetism and spintronic applications [73].

Graphite structure consists of planar layers of sp^2 hybridized carbon atoms forming a virtually infinite horizontal hexagonal array. The interlayer distance is 3.347 Å and the distance between carbon atoms within each layer is 1.418 Å. The planar layers are held together by weak non-covalent forces (stacking interactions). The two known forms of graphite, alpha (hexagonal) and the energetically less stable and less common beta form (rhombohedral) differs for the graphene layers stacking (ABA and ABC stacking in alpha graphite and beta, respectively) but exhibit comparable physical properties. The two forms can interconvert upon mechanical treatment (alpha to beta) or by heating above 1300 °C (beta to alpha) [70, 72, 74]. Because of this peculiar structure, the graphite is strongly anisotropic and acts as a conductor in the direction of the planes, and as an insulator perpendicularly to them. The planar structure of graphite allows electrons to move easily within the planes leading to high electrical and thermal conductivities [72]. The weak interplanar forces allow the possibility for certain chemical species (atoms, molecules and ions) to intercalate into the interplanar spaces of the graphite generating expanded graphite and a variety of graphite intercalation compounds (GICs) [75, 76].

Graphite is one of the strongest materials known per unit weight: the theoretical Young's modulus of an individual graphene layer is 1600 GPa. Graphite conducts electricity and heat as well as absorb light (it appears black in color). Graphite has a low density (2.266 $g \cdot cm^{-3}$) and the theoretical surface area of a planar layer is 2630-2965 $m^2 \cdot g^{-1}$. In the case of synthetic graphite, the properties depend of course from the synthetic conditions applied [70, 72]. However, the weak bindings between the carbon layers that are joined together via weak van der Waals forces makes graphite soft and slippery, and suitable to be used as a lubricant or in pencils and as starting material for the production of other graphene related materials by mechanical and chemical routes.

2.6 Graphene

Graphene was described for the first time in 2004 as monolayer and crystalline graphitic films by Andre Geim and Konstantin Novoselov [77]. Its discovery allowed the two scientists to be awarded by the Nobel prize for Physics in 2010. It is the thinnest and strongest honeycomb lattice structure composed of carbon atoms [78, 79]. It is widely regarded as a building block of many other CNM, such as fullerenes, CNT or graphite.

Graphene is a 2D single layer of sp^2-hybridized carbon atoms arranged into a honeycomb lattice with C-C bond length of only 0.142 nm. It is characterized by unique structural, physical and mechanical properties. Graphene exhibits high electrical and thermal conductivity, optical transmittance, Hall and tunneling effects and bipolar electric field effect [78]. Graphene is considered as a zero-overlap semimetal or zero-gap semiconductor with very high electrical conductivity. The maximum electron mobility of graphene at room temperature can reach $2x10^5$ $cm^2(V \cdot s)^{-1}$ and thus the ideal conductivity of graphene is over $1x10^6$ $S \cdot cm^{-1}$ [78]. From the mechanical point of view graphene exhibits high strength, good elastic properties and high Young's modulus [80]. Table 1 reports a list of the main properties of graphene. Graphene is also characterized by high surface area, hydrophobic behavior, it exhibits chemical inertness and gas impermeability. Nevertheless, some types of graphene, depending on the synthetic strategy applied, are prone to be functionalized. The graphene toxicity is currently under study and it was found to be dependent on the synthetic approaches. Even though most graphene and its

derivatives show potential toxicity in biological systems, some studies report that pure graphene is biocompatible [81].

Table 1 List of graphene's main properties.

Properties	Value
Density	0.77 mg·m^{-2}
Melting point	3800 K
Specific surface area	~2600 m^2·g^{-1}
Transmittance for visible light	97.9 %
Thermal conductivity	3-5 10^3 W(m·K)$^{-1}$
electrical conductivity	10^2 - 10^6 S·m^{-1}
Current density	>10^9 A·cm^{-1}
Electron mobility	> 10^5 cm^2(V·s)$^{-1}$
Young's modulus	1100 GPa
Tensile strength	~1.5 TPa
Breaking strength	42 N.m^{-1}
Elastic limit	~20 %

Graphene synthesis is carried out by different methods that can be gathered into two main categories: top-down and bottom-up approaches [79, 82, 83]. The top-down approach is carried out starting from a graphitic material (pure graphite or other CNMs) while bottom-up approach allows to produce graphene starting from low molecular weight species (hydrocarbons and silicon carbide, SiC). Broadly speaking, the bottom-up approach is quite simple, but it produces desired material in low yield and requires very high temperature to operate. In addition, bottom-up techniques need expensive equipment and require specific metallic substrates on which high quality graphene, yet in limited quantities, is grown. Top-down approaches separate the stacked sheets by disrupting the van der Waals forces that hold the graphene sheets together and allow isolating multilayer defective graphene sheets. Top-down approaches include mechanical exfoliation, electrochemical exfoliation, solvent-based exfoliation, electrochemical and chemical reduction strategy, arc discharge, and unzipping of carbon nanotubes. While the bottom-up approaches include epitaxial growth on SiC, CVD, substrate-free method and carbonization [79, 82, 83]. In Table 2, the main synthesis methods employed, the precursor, their advantages and shortcomings are listed [79, 82, 83].

Table 2 Summary of the methods used for graphene preparation [79, 82, 83].

Technique	precursor	Type of method	Graphene properties	Advantages	Drawbacks
Chemical vapor deposition	Hydrocarbons	bottom-up	High quality graphene Production of single layer graphene.	Large area (up to ~1 cm^2) are achievable. Limited number of defects.	Transfer of graphene films deteriorates graphene quality and causes wrinkle formation. Poor scalability. Expensive.
Epitaxial growth on metal	SiC	bottom-up	High quality graphene. Few defects. Rarely a number of layers ≤2 is achievable.	Large area (up to ~1 cm^2) are achievable. Limited number of defects.	Requires high temperature, expensive and difficult transfer process. Not feasible at commercial level. Possible transfer of graphene from SiC substrates.

Arc discharge method	Graphite	top-down	Pure graphene cannot be obtained	Applicable to obtain Boron or nitrogen doped graphene.	Not scalable.
Wet chemical synthesis (oxidation through Hummer, Brodie methods followed by Reduction of GO)	Graphite	top-down	Transparent conductive films are achievable. Useful to synthesis graphene-based composites.	Economical and facile technique.	Presence of oxygen impurities. Not suitable for most of the electronic applications. Can be obtained in lab but not good enough for commercialization. Significant number of defects.
CNTs unzipping	CNTs	top-down	Few-layer graphene	Scalable with controlled widths and edge structures. Better control over chemical functionalizatio n and edge quality.	Low yield. More expensive in respect to chemical exfoliation of graphite or graphite oxide.
Mechanical Exfoliation	Graphite	top-down	High quality graphene. Few defects. yields mono-, di-, and few-layer graphene.	Inexpensive. Simple process.	Flakes randomly distributed, poor yield. Not scalable. Poor reproducibility. Not amenable for large scale production. Slow method, used mainly at laboratory scale
Liquid-based exfoliation	Graphite	top-down	Low quality graphene	Simple process.	Expensive and hazardous solvents or surfactant molecules are difficult to remove and affect properties of graphene (including overall biocompatibility). Increased concentration of graphene is accompanied by the decrease in flake size and increase in defect contamination.
Electrochemical exfoliation	Graphite	top-down	High quality graphene, low quantity of oxygen.	Promising bulk method. Suitable for graphene nanocomposite s/hybrids production.	Produces a mixture of different thicknesses of graphite flakes with the possibility to isolate few-layer graphene by centrifugation. Surfactant molecules are difficult to remove and influence the electrical and electrochemical properties of graphene.

Among the different chemical methods, wet chemical synthesis through graphite oxide (GO) as precursor of graphene-based materials is one of the most widely used protocol. In general, such approach involves the chemical oxidation of natural graphite using various solution-based routes, an exfoliation step (e.g., using ultrasonication) to isolate few layer graphene oxide sheets and then their thermal/chemical/electrochemical reduction to produce reduced graphene oxide (rGO) (more details find bellow [84]. The graphene resulting from chemical approach has limited solubility or even undergoes irreversible agglomeration during preparation in water and most organic solvents, owing to the strong π–π stacking tendency of rGO sheets [84]. CVD and micromechanical exfoliation of graphite are the most widely used fabrication methods of less defective graphene films [85, 86]. However, the CVD direct deposition of uniform graphene films on arbitrary substrates at low temperatures is not

possible and furthermore this method is incompatible with mass production processes or with delicate substrates [86]. The exfoliated graphene exhibits poor solubility in common organic solvents due to the addition of a stabilizer as the exfoliation liquid medium [85].

Graphene finds applications in the fields of sensors, energy storage devices, fuel cells, high-strength materials, optoelectronic devices, and batteries. Recent applications include its use as armor material, for biomaterials production, in bionics, and in the biomedical sector for therapy, diagnosis and drug delivery [87-92].

It should be noted that the single-word "graphene" is now being used in the literature to refer to a wide variety of materials, that not always correspond to a mono layer graphene. According to Bianco et *al.* [93] when the number of stacked graphene layers increases from more than one, these particles should be referred as bilayer and trilayer graphene (for 2 or 3 layers), few-layers graphene (FLG) (between 2 and 5 layer), multi-layer graphene (MLG) (between 2 and about 10 layers) and graphite nanoplates (GNP) (above 10 layers and below 100 nm thickness). Based on these terminology and guidelines, the term graphene nanoplatelets, very mentioned in the literature, is not recommended [93]. Also, the physical properties that make graphene such an exciting material, deteriorate rather rapidly with the number of stacked layers [94]. For instance, Gong et al. [95] reported Young's modulus decreases from 1 TPa to ~600 and 400 GPa when going from an monolayer graphene to FLG and MLG of 5 or 10 layers, respectively.

2.7 Graphene oxide (GO)

Graphene oxide (GO) is a two-dimensional material with hexagonal carbon structure similar to graphene. It can be considered as the oxidized form of graphene, with oxygen-containing functional groups decorating the sp^2 basal plane and the edges. The typical oxygen-containing groups in GO are: hydroxyl (–OH), epoxy, carbonyl (C=O), carboxylic acid (–COOH), lactone and phenolic groups [96-98]. GO contains both aromatic (sp^2) and aliphatic (sp^3) domains randomly distributed within the graphene oxide layered structure and the relative size of these two regions depends on the degree of oxidation (Figure 2).

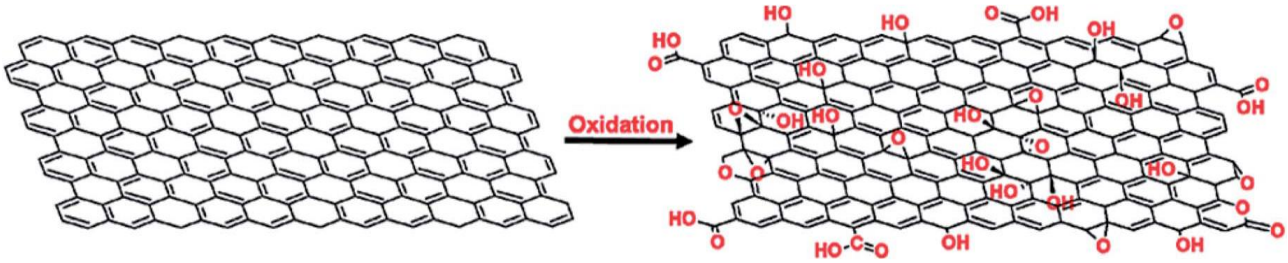

Figure 2 Graphene oxide structure [96].

Lerf and Klinowski [99] proposed a structural model of GO, known as the L–K model, which described GO as made by not oxidized aromatic patches of variable size, separated from each other by aliphatic 6-membered rings decorated with functional groups lying both above and below the basal plane. In particular, hydroxyl and epoxy groups were randomly distributed on the GO single layer, while the carboxyl and carbonyl groups were distributed at the edge of the single layer [98, 99]. Erickson et *al.* [100] studying GO *via* SEM, assessed that this particle is not only characterized by disordered oxidized regions and unoxidized aromatic regions, but it also contains hole defects due to over-oxidation and lamellar peeling.

Due to the presence of a large number of oxygen-containing functional groups, GO is hydrophilic and it can be easily dispersed in water solution, generating brownish appearance solutions with unique mechanical, colloidal or optical properties. Generally, GO water suspensions are characterized by high

colloidal stability [101]. Even though GO is most commonly dispersed in water, it can be also dispersed in organic solvents [102], where the GO sheets are negatively charged to become a colloidal suspension stabilized by electrostatic interactions.

GO is characterized by a great variability in terms of dimensions and C/O ratio: these two aspects depend on the domain size of the starting graphite, the oxidation time, and the type of oxidation procedure [96]. GO flakes obtained at the end of oxidation are typically irregularly shaped and their size can vary from a few nm to mm [97]. The average lateral size of the GO flakes can be easily tuned by sonication: flakes dimensions are thus reduced by means of repeated fragmentation. The thickness of the GO flakes is another relevant morphological parameter. The AFM measured thickness of a single layer GO flake typically ranges between 1.0 nm and 1.4 nm [97, 103], well above the values of thickness typically measured for graphene (0.35 nm) due to the presence of oxygen-containing functional groups protruding out of the basal plane. Since the process leading to the production of GO results in disruption of the aromatic network of graphene layer and in the introduction of functional groups that inhibit its electrical conductivity, GO behave as high electrically resistive materials (resistivity around 1.6 x 10^4 Ω·m). In addition, GO exhibits also a low thermal conductivity of 0.5-1 $W(m \cdot K)^{-1}$ [104].

GO can be produced in desirable quantities rather rapidly and at low cost by different methods. High-quality GO can be easily produced from graphite flakes using well established chemical or electrochemical exfoliation methodologies. The chemical routes are based on protocols deriving from the modification and the improvement of previous approaches proposed by Hummers, Staudenmaier, Brodie. For instance, Hummers and Offeman significantly improved the original Brodie's protocol, introducing the use of potassium permanganate ($KMnO_4$) as an oxidizer instead of potassium chlorate ($KClO_3$), which evolves toxic chlorine dioxide (ClO_2) gas and the use of sodium nitrate ($NaNO_3$) in the place of concentrated nitric acid (HNO_3) solutions [96, 104, 105]. The most used modification of this approach is probably the "improved Hummers' method". This method uses a combination of phosphoric acid (H_3PO_4) and $KMnO_4$ (at higher extent with respect to the classical Hummers' method) instead of sodium nitride. This improvement allows to significantly reduce the toxic gases evolution, provides an easier control of the reaction temperatures, and results in GO powders with a higher degree of oxidation [106]. A comparison among these GO chemical methods is reported in Figure 3.

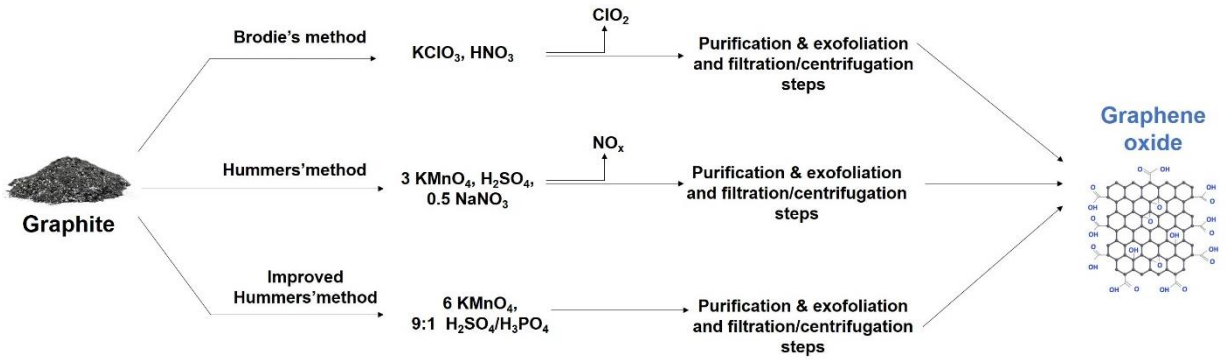

Figure 3 Comparison among the main chemical protocols to produce GO.

Graphite can also be oxidized prior to GO synthesis to decrease the C/O ratio of the final product. The method proposed by Kovtyukhova et *al.* [107] required a graphite pretreatment with potassium persulfate ($K_2S_2O_8$) and phosphorus pentoxide (P_2O_5) prior to use in the Hummers' method. Other researchers prior modified graphite into expanded graphite by thermal treatment or exposure to strong oxidizers to increase its interlayer spacing, resulting in easier delamination of the graphite oxide layers [108].

Recently, novel and greener approaches for GO synthesis have been proposed [96, 104]. For example, Yu et al. [109] reported a method based on iron-induced procedure in absence of acid media, while Peng et al. [110] as well proposed a Ferrate-based procedure, but the use of H_2SO_4 was necessary.

The tunability of both GO oxidation degree and flakes combined with its easy processability, make GO an appealing material in many fields: electronics (sensors and transparent conductive films), composites materials (multifunctional gels, materials for water purification), clean energy devices (solar cells, supercapacitors), biology and medicine (for generation of neurons, cellular migration, drug delivery) applications. GO can be easily deposited by drop casting, dip coating, spray coating, spin coating, Langmuir-Blodgett (LB) technique, and vacuum filtration to produce good quality films and membranes [96, 104].

2.8 Reduced graphene oxide (rGO)

Reduced graphene oxide (rGO or RGO) possesses a heterogeneous structure comprised of a graphenic layer populated with structural defects and residual oxygen-containing functional groups [84]. rGO is quite easy to prepare with high yield from GO by using a variety of chemical, electrochemical, thermal, and microwave- and photo-assisted reduction methods. Each different reduction process leads to rGO differing in morphology, mechanical, optical and electrical properties. The differences depend also on the reduction degree. The key design factors in GO reduction include the C/O ratio of the end product, selectivity in removing a single type of oxygen group (hydroxyl vs carboxylic acid vs epoxy, etc.), healing of the surface defects of the GO from oxidation, and choice of green reducing agents. In addition, the different methods provide different advantages in scalability, energy usage, and amount of chemical waste produced [84, 104].

The use of chemical reducing agents to obtain rGO solutions is the most common reduction technique being hydrazine [111], metal hydrides and hydrohalic acids [112] the most commonly used reducing agents. Recently, a number of “green” reducing agents have been proposed, such as ascorbic acid, sugars, amino acids, and even microorganisms [112].

The thermal reduction is performed by annealing GO at elevated temperatures in an oxygen-free environment [113] or by less-conventional methods such as microwave assisted reduction or flash reduction of GO films by high-intensity light [114]. rGO can also be synthesized through photocatalyzed reactions, for instance by the reduction of GO film using UV light in the presence of a titanium dioxide (TiO_2) catalyst [115]. Electrochemical reduction doesn't require the use of chemical agents since the reduction process is driven by electron exchange between GO and the electrodes of a typical electrochemical cell [116].

rGO exhibits mechanical, optoelectronic or conductive properties similar or comparable to those of graphene. Upon reduction, the electrical conductivity of GO can be greatly improved up to conductivities ranging from ~0.1 $S \cdot m^{-1}$ to $3x10^4$ $S \cdot m^{-1}$ [84]. The conductivity is not so high as that of graphene because, even after reduction, rGO contains holes (as a consequence of the oxygen-containing groups removal) and defects including residual sp^3 bonded carbon to oxygen, which disturbs the movement of charge carriers through the aromatic area. As matter of fact, electrical transport in rGO occurs primarily by hopping, which differs from that of mechanically exfoliated graphene [84]. rGO presents not only good absorption properties over the whole spectrum (even a single-layer of rGO can absorb a significant amount of light in the visible and near infrared range), but it also possesses functional groups that could make it dispersible in a variety of solvents of interest. It is worth noting that rGO tends to aggregate during the reduction process and therefore much research efforts are dedicated not only to the optimization of the GO reduction process but also to stabilization of rGO immediately after the reduction [84].

rGO finds application in many fields. Sensing, biological, environmental or catalytic applications as well as optoelectronic and storage devices involving rGO have been widely reported recently in the literature [84, 104].

2.9 Graphene nanoribbons

Graphene nanoribbons (GNR) are also considered quasi-one-dimensional (1D) structures because of a great disparity between their lengths and widths. GNR are long and narrow planar strips of graphene whose width is less than 50 nm. Similar to CNT, the graphene's honeycomb structure provides two distinctive edge geometries: zig-zag and armchair, while chiral GNR have both zig-zag and armchair parts along the edges [117, 118]. Their electronic and optical properties are determined by their chemical structure which implies their width and edge configuration. The zig-zag GNR manifest metallic properties, while armchair GNR can have either semiconducting or metallic properties [119]. For sensing applications of GNR, an important step is to tune their bandgap which could be conducted by controlling the parameters such as width, crystallographic symmetry, edge structure, strain, and doping with heteroatoms [120].

Similarly, to other CNM, GNR are generally chemically inert and do not form stable dispersions in the most commonly used solvents. However, due to their large surface area, physical adsorption of various molecules or nanoparticles occurs at GNR surfaces [121, 122]. The dangling bonds located at the edges of GNR enable their chemical modification by functionalization with various functional groups. GNR can be oxidized to introduce oxygen-functionalities at the basal and edge planes which, in addition to their wide bandgap and large surface area, make GNR suitable candidates for sensing molecules that have high oxidation potentials [123]. One or more carbon atoms from graphene lattice can be substituted with a heteroatom which induces changes in GNR' electronic properties. Those changes can be tuned by the type and density of dopants, and their position at the lattice [124, 125].

There are several methods to produce GNR. Among them are longitudinal unzipping of CNTs [126] and cutting of graphene by lithography [127] as top-down methods, or CVD [128] as the bottom-up method. The main obstacle to the larger-scale utilization of GNR is the preparation of GNR with defined and narrow widths and smooth edges in larger quantities. To date, the highest quality of GNR was achieved by the unzipping of high-quality CNT and cutting of high-quality graphene, while the CVD method provides grams-per-day quantities of GNRs [119].

2.10 Graphene-like materials

Recently many attempts to produce graphene-like materials starting from sources different from graphite have been formulated. For instance, Alfè and coworkers [129, 130] in the last ten years focused their efforts in the characterization and the utilization of graphene-like layers (GL) obtained through two steps oxidation/reduction approach involving a severe destructuration of a furnace carbon black (CB) (90 h of hot acidic treatment). In particular, the destructuration of the CB microstructure led to the isolation of two classes of water-stable materials: i) GL and ii) small graphenic fragments classifiable as carbon nanodots (CDs) exhibiting fluorescence in the visible region. After the oxidation step, graphene like layers in a highly oxidized form (GLox) were isolated and then chemically reduced and stored in aqueous suspension [129, 130]. The CB-derived GL materials are made up by stacked short graphenic fragments (the vertical sizes range from about 1 nm or less to a few nanometers while the larger lateral dimensions are a few tens of nanometers) characterized by a residual functionalization at the edge but not at the graphenic basal planes. Infrared and X-ray photoemission spectroscopy inspections indicated that the edges of the basal planes of CB-derived GL are decorated mainly by oxygen-containing functional groups (mainly carboxylic and carbonyl groups) [129, 130]. A more precise classification and

quantification of the main oxygen-containing functional groups was achieved by Coulometric–potentiometric titration in the pH range 2.7 < pH < 7 [130]. The presence of such a complex variety of oxygen functional groups allows for an exceptional colloidal stability over a wide pH range (3-14) without the use of any surfactant. CB-derived GL exhibit a peculiar self-assembling behavior when dried on surfaces, as a consequence of the suspension pH, surface roughness and chemistry [130-132]. All these peculiar characteristic of CB-derived GL make them particularly suitable for the preparation of a wide array of hybrid materials including intercalated metal organic frameworks (MOFs) [133, 134], biocompatible interfaces [132, 135, 136] and photoactive materials [137]. CB-derived GL are also particularly suited to homogenously coat non-planar surfaces as living cells [138] and they exhibit no toxicity in vivo, since they do not lead to any perturbations of different biological parameters on the vertebrate model Danio rerio (zebrafish) [139]. The quite good conductivity of films of CB-derived GL ($2.5 \pm 0.3 \times 10^{-2}$ S·cm^{-1}) was exploited in the production of conductive hybrid materials [132-136] and in the preparation of prototypal chemoresistive sensing devices (by drop casting and inkjet printing) for the detection of alcohols vapors in the range of 0-100 ppm [131, 140].

2.11 Bio-based CNM

Climate change and global warming continue to threaten all living things in the world, especially biodiversity. In order to stop climate change, the world has to limit the use of fossil-derived carbon resources and stop it as soon as possible. In this sense, each sector seeks to find alternative green solutions by using high technology related to its own process. Many branches of industry, especially the automotive, aerospace and defense sectors, always payed attention to using the most advanced technologies, and the desire to benefit from composite materials is increasing. Sustainability of composite materials for high performance applications is an important issue in modern processing technologies.

In this sense, research has moved towards the attempt to produce carbon nanomaterials and graphene-like materials from alternative sources, such as waste biomasses and bio-precursors. For instance, lignocellulosic biomass, the most abundant organic material on earth, has been recognized to promising alternative green carbon resources. Interest in "biochar" or “biocarbon”, the solid residue of the thermal (pyrolysis) transformation of lignocellulosic biomass, is increasing. In the newly released biochar market report, it is estimated that the biochar production in the world in 2026 will be 2 billion USD [141]. Biocarbon is the most cost-effective area for the development of next-generation functional carbon materials. As a stand-alone material or as a component in composite materials, biocarbon has proven its effectiveness and usage advantage in many areas from environmental improvement to sustainable energy. Every ton of biochar to be used instead of fossil derivatives will create a carbon sink, preventing one tonne or less of the equivalent CO_2 from re-entering the atmosphere. The heterogeneous structural properties of biomass precursors and the production methods used play an important role on biocarbon properties. When the economic and environmental pollution problems in the world are taken seriously, research in this field have intensified [142, 143].

Typically, carbon nanomaterials are produced from biomass via pyrolysis, including salt-based activation, chemical blowing, or the coupling with hydrothermal carbonization pretreatment, post exfoliation, and some other methods [144]. The activation processes using salts can be applied directly to the biomass or to the biocarbon after pyrolysis to produce the activated biocarbon with high yields. The use of potassium hydroxide (KOH) has been proven to be particularly effective in creating micropores and increasing the specific surface area of these products [145-148]. Also, many works demonstrated that the coupling with hydrothermal carbonization is determinant for graphitic region formation since the direct pyrolysis leads to an amorphous phase with a very graphitization degree [144]. Moreover, the salt-based method and the pyrolysis coupled with hydrothermal treatment

methods are widely applied and show great advantages in scalability compared with other methods [144]. Mechanical force (ball milling) and mechanical exfoliation (sonication) are favoured techniques from researchers to maximize the surface area of the biocarbon. There have been some studies where ball milling was applied both after pyrolyzed [149-151] or activation process [152, 153]. Peterson et al. [154] investigated the effect of ball milling parameters on surface area of biocarbon, denoting great influence on the quantity of solvent used. The types of biomass mostly used for the preparation of bio-based carbon and GL materials are rice husk, empty fruit brunch, sugar cane bagasse, mango peel, pine bark, peanut shell, populous wood, among others [155, 156]. Recent studies on bio-based carbon materials derived from biomass are summarized in Table 3.

Table 3 Recent studies on bio-based carbon materials.

Product name	Biomass type	Manufacture technics	Surface area or particle size	Application	Ref
Biocarbon	Miscanthus fibre	Pyrolysis at 650 °C and 900 °C and ball milling (2h)	300 $m^2 \cdot g^{-1}$ (650 °C) 3.81 µm (900 °C) 4.26 µm (650 °C)	Filler in PP polymer matrix	[149, 150]
		Pyrolyzed at 650 °C *industrial ball milling for 24 hours ** industrial hammer milled	* 0.9 µm ** 20-75 µm	Filler in PLA polymer matrix	[151]
Activated Biocarbon	Miscanthus fibre	Pyrolysis at 700 °C - Activated with KOH at 900 °C for 1 h	BC: KOH (1:4) 3024 $g \cdot m^{-2}$	High-performance EDLCs (Electric Double Layer Capacitor)	[157]
Bionanocarbon	Oil palm shells	KOH impregnation 4h 120 °C - carbonization 700 °C 30 min-high energy ball milling 24 h	Average 81.4 nm	Nonwoven Kenaf Fibre vinyl ester Nanocomposites	[158]
				Propionic Anhydride Modified Kenaf Fibre with Bionanocarbon in Nanobiocomposites	[152]
		NaOH impregnation 4h 120 °C - carbonization 700 °C 30 min-high energy ball milling 24 h	Average 74.81 nm	Modified kenaf bast fibre with propionic and succinic anhydrides-vinyl ester nanocomposites	[153]
Nano Bio charcoal	bamboo	solution casting method	624.81 $m^2 \cdot g^{-1}$ 69.43 nm (Particle diameter)	Nanofiller in PVA nanocomposites	[159]
Bio-few layered graphene	waste peanut shell	Pyrolyzed at 800 °C for 2h, activated at 800 °C with KOH for 2h- 10 % H_2SO_4 aqueous solution through probe sonication for 1 h (mechanical exfoliation method	2070 $m^2 \cdot g^{-1}$	Supercapacitor device	[160]
Graphene like nanosheets	Coconut shell	simultaneous activation ($ZnCl_2$) – graphitization ($FeCl_3$) at 900 °C for 1 h	1874 $m^2 \cdot g^{-1}$	Supercapacitors	[161]

Chitosan bio-modification of a carbon nanotube (CNT) arrayed electrode	Chitosan from shrimp shells	Bio-fabrication: coated CNT arrayed electrodes with thick chitosan films	-	Selectivity of electrochemical sensors in multicomponent biofluids	[162]
Bio-oil based carbon nanotubes cotton (Bio-CNTC)	waste cooking palm oil	Thermal CVD (TCVD) furnace scaled-up prototype	Ranging from 19.5 to 36.2 nm	Composite material, especially CNT/natural rubber-latex (NRL) nanocomposite, supercapacitor application.	[163]
		A horizontal tubular FCCVD reactor and hybridization ZnO chemical bath deposition method	64 nm Bio-CNTC 44 nm hybridize CNTC with ZNR	Comparable to other substrate such as glass and silicon	[164]
Biocompatible non-toxic materials	Cellulose paper	PPy/CNT composite deposited on cellulose paper	24.65 $m^2 \cdot g^{-1}$	Implantable bio-electronic cells	[165]
Carboxymethyl cellulose (CMC)	cellulose	bio-nanocomposite films via solvent casting method	N/A	CMC/HNT bio-nanocomposite films CMC as a matrix HNT as a filler	[166]
Carbon nanoparticles with high surface area from lignin	Lignin	-lignin by sublimation process (impregnation with KOH and freeze drying) -Thermo-stabilization and carbonization of sublimated lignin	42 $m^2 \cdot g^{-1}$	Carbon nanoparticles as high value-added products	[167]

Due to its high carbon content, plastic wastes can also be considered a feedstock of choice for the production of GL materials allowing for the identification of innovative, promising and more environmentally sustainable CNM production routes. The main results on such a topic have been recently reviewed with the aim of highlighting the current advances in wastes-derived graphene synthesis, identifying the synthetic difficulties encountered and to be faced in the next future and of predicting the future development in such research field [168, 169]. Monolayer, few-layer and multi-layer graphene (including flash graphene) can be obtained from plastic wastes through many synthesis methodologies: (i) pyrolysis of the plastics directly over a metal substrate or in presence of a catalyst; (ii) CVD on a metal substrate using hydrocarbons evolving from the thermal decomposition of the plastics; (iii) thermal decomposition followed by ball milling and microwave sintering; and (iv) flash Joule heating (FJH) [169].

Similarly, bio-precursors, including glucose, xylitol, sucrose, caramel, chitosan, alginate, white straw, palm oil, allowed for the production of graphene-like materials by classical thermal methods (pyrolysis, carbonization, graphitization), chemical treatments (chemical activation), hydrothermal methods, template-based confinement method and combined approaches based on hydrothermal treatment and graphitization, chemical treatment and pyrolysis or carbonization [170]. Some preparation approaches required also the use of clay, sepiolite, oxides or metal salts as synthetic aid [144, 156]. In some cases, also the CVD on a metal substrate of products evolving from the thermal decomposition of bio-precursors are proposed [155].

Recently, Sierra and coworkers [171-173] performed studies on the production of GL materials using coke (a product derived from coal). In one of their earlier studies, two carbochemical cokes and a

petrochemical one were oxidized and the resultant oxidized products exfoliated by ultrasound to yield graphene oxide materials [172]. These coke-derived GL materials exhibited characteristics similar to those graphite-derived, while the size of the sheets was larger [172]. The last approach they proposed was mechanochemical, where oxidative treatments were avoided by ball-milling of coke in presence of stearic acid [173]. They obtained GL products with high yield after one hour milling by using a 2:1 mixture in weight of stearic acid and coke. Stearic acid acted as a lubricant and exfoliation aid and also prevented material oxidation. Atomic force microscopy (AFM) revealed that the obtained product was made up by few-layer stacked sheets with lateral sizes ranging between 1-3 μm [173]. This approach, due to the ample availability of the precursors, the low cost of the technology exploited and absence of toxic reagents, represents a green method for manufacturing few-layer GL materials in one step and good yield. Saha and coworkers [174] also proposed the production of graphene-like materials from petroleum coke by electrochemical exfoliation after an oxidative treatment of coke and the obtained product was further annealed to get an improved electrical conductivity. The morphological, compositional and structural analyses performed on the final product confirmed that the production of GL material in form of few-layered nanosheets [174].

Different types of multi-layered GL materials (biocarbon, activated biocarbon, bio-graphene and bio-oil based CNT, among others), have been produced from bio-precursors, biomass and wastes and exhibit high surface area, porous structure, high graphitization degree and chemically stable surfaces. These materials find a wide range of applications, including supercapacitors [157, 160, 161, 163], filler in bio-composites [149-151], nanocomposites [152, 153, 158, 159], biosensors [162, 175], advanced energy storage [176], conductive coating, etc [144, 155, 156, 170].

Generally, the quality of these materials obtained by unconventional sources is highly dependent on the feedstock, manufacturing techniques and fabrication conditions applied. Giving this, efforts should be made in the direction of a unified technological standard or grading system for graphene-like structures and overall performances. Moreover, the manufacture and application of these materials still needs investigation to guarantee a maximization of these promising materials.

According to this extensive overview, it can be stated that carbon nanoparticles present outstanding advantages that make them attractive as fillers for different sensing applications. However, from a practical point of view, there are many challenges to be overcome regarding the incorporation and dispersion of CNM for developing novel materials. Therefore, in the following sections, guidelines and good practices referring to the manufacturing processes of CNM composites will be explored in more detail.

3 Thermoset-based composites

Modified polymer nanocomposites with conductive CNM have recently attracted great interest in nanotechnology and materials science. For the design and manufacturing of advanced composite, epoxy is one of the most widely used conventional thermoset polymers. Owing to its high specific strength, stiffness, dimensional stability and chemical resistance, among others, epoxy resin has been increasingly used in highly demanding fields [177]. For instance, for aeronautic, aerospace and automotive applications, epoxy-based carbon fibre reinforced polymer composites (CFRP) are substituting structural metal components due to its high strength-to-weight ratio, offering great impact in the reduction of fuel consumption and gas emissions, and easy processability into complex structures [178]. The addition of CNM to the epoxy resin, giving rise to modified suspensions that are further used for producing multiscale CFRP, has been highly desirable not only for the improvement of the brittle and insulating nature of the polymeric matrix, but also the interface between the carbon fibre and the matrix. Moreover, further multifunctionalities are able to be introduced in the modified materials, enabling its use for electromagnetic interference (EMI) shielding and sensing applications, among others [177].

3.1 Difficulties to disperse CNM in thermoset matrices

As previously mentioned, CNMs present outstanding features but it is common to observe a discrepancy between theory and practice when it comes to modified composites, since the final properties of the materials are strongly dependent on the fabrication process and, in particular, by the dispersion state of the nanofiller and the interfacial adhesion between the particles and the matrix. Depending on the geometric features of CNM, the high surface area associated to the presence of van der Waals forces or π-π stacking, typically causes a strong agglomeration of CNM [179, 180]. In fact, one of the most technical challenges for the design and manufacturing of particle-reinforced composites with improved properties and multifunctionalities is the presence of agglomerates, and the difficulty to achieve homogeneous dispersion and stability, especially considering the desired formation of a conductive network to attain higher sensitivity for different sensing applications, while not fatally compromising other properties of the matrix. Therefore, researchers have been investigated different approaches to solve this and other problems associated with the properties of modified polymer composites [181, 182].

3.2 Strategies to maximize properties of CNM in thermoset nanocomposites

According to the International Union of Pure and Applied Chemistry (IUPAC), dispersion refers to a system in which distributed particles of one material are individually dispersed in a continuous phase of another material. At the same time, this term also indicates procedures used for the introduction of such particles in a continuous phase. CNM can be dispersed in thermoset matrices using different methodologies and approaches, which are mainly divided in: i) mechanical (mechanical stir, ultrasonication and/or calendaring) and ii) chemo-physical (chemical and physical functionalization) [181, 182]. It is important to note that both these types of methodologies can be combined to promote higher levels of dispersion of the particles in the matrix and to improve interfacial bonding between both.

3.2.1 Ultrasonication

Ultrasonication is an effective method widely exploited to disperse fillers in liquids having a low viscosity. This technique can be performed either by using ultrasonic bath or an ultrasonic probe/horn, also known as a sonicator. Ultrasonication is based on the cavitation mechanism, which consists in the formation of high energy bubbles that collapse within the liquid and generate a wave-shock, providing high energy local shear and promoting the ‘‘peeling off” of individual nanoparticles located at the surface of nanoparticle bundles or agglomerates [181, 182]. Commercial probe sonicators have an adjustable amplitude ranging from 20 to 100 % and a power of 100–1500W. In this technique, and due to the viscosity of the thermoset matrices, the nanofillers are often dispersed in a solvent, such as water, acetone and ethanol, which is subsequently mixed with the resin and evaporated. Due to the substantial heat generated by ultrasonication, it is also common to use an ice bath to prevent the solvent evaporation. According to the literature, several authors report the use of bath sonication or ultrasonication to successfully disperse carbon-based nanoparticles into thermoset matrices, such as SWCNT and MWCNT [183-189], CNF [190-192], multilayers graphene/GO/rGO [193-200].

For instance, Esmaeili et *al.* [201] prepared epoxy nanocomposites containing 0.25, 0.5, and 0.75 wt. % SWCNT and CNT using sonication for 30 min with an amplitude of 50% to break the aggregates. Best electrical conductivity and mechanical results were achieved for lower CNT loadings. Bouhamed et *al.* [202] carried out studies on the effect of sonication and curing time on the properties of nanocomposites containing MWCNT, and the results showed that sonication time bellow 25 min resulted in samples containing poorly dispersed CNT, with the presence of large aggregation. Better homogeneity and uniformity were observed above sonication time of 30 min. Kumar et *al.* [203] reported an approach to achieve homogeneous dispersion of CNTs in the polymer matrix by applying simultaneously ultrasonic waves and shear force generated by axial flow impeller. Field Emission Scanning Electron Microscopy (FESEM) studies confirmed cluster free uniform dispersion of MWCNT in epoxy matrix, which lead to enhanced tensile strength by 35 %, toughness by 53 % and storage modulus by 35 % with a loading of 0.75 wt. % CNTs. On the contrary, Tang et *al.* [204] reported that better dispersion was achieved for modified nanocomposites by first dispersing RGO into ethanol and ultrasonicating for 2 hours followed by planetary ball milling. The produced nanocomposites presented fracture toughness increase of 52 % over the neat epoxy and electrical conductivity 2 orders of magnitude higher than the poorly dispersed graphene for 0.2 wt. % incorporations.

From an industrial point of view, the required used of high quantities of solvents, plus the additional steps to guarantee its complete evaporation, is not desirable not only due to costs, but also having in mind environmental concerns [205]. More recently, several authors reported the use of ultrasonication without the use of solvents. Frømyr et *al.* [206] studied the effect of different ultrasonication conditions on the direct dispersion of MWCNT into an epoxy hardener (methyl tetrahydrophthalic anhydride, MTHPA). The results showed that increasing the dispersion time or acoustic intensity of the sonication had a positive effect on the quality of the dispersion, by increasing the mass fraction of the free and un-entangled nanotubes. However, at 70 % amplitude, unwanted side effects were detected, namely the degradation of the curing agent. It should be noted that this authors also added a block copolymer (BYK D2105) to further aid the dispersion of the CNT in the epoxy hardener. Gkikas et *al.* [207] also investigated the effect of sonication duration and amplitude on the mechanical properties of nanocomposites modified with MWCNT (sonication performed directly in epoxy mixtures with CNT). Fracture toughness enhancements of 250 % were achieved for 2 hours of sonication and 50 % sonication amplitude, while the use of 100 % amplitude for both 1.5 and 5 hours resulted in fracture toughness decreases. An and Jeong [208] also used ultrasonication to directly disperse graphene sheets into an epoxy resin for the production of composite films. The produced materials presented decreased electrical resistance from around 10^{13} Ω to 10^{3} Ω with the increasing graphene content.

Even though good results were reported with the application of this methodology, it is important to notice that if the sonication treatment is too aggressive and/or too long, the fillers can be easily and seriously damaged [209]. Through RAMAN spectroscopy, for instance, it is possible to determine surface damage of CNT after sonication on the changes of characteristic bands: D-band at 1340 cm^{-1} is a defect-induced feature attributed to disordered sp^3 carbon on CNTs; G-band at 1580 cm^{-1} related to in-plane vibrations of the graphene layers (this band is independent of the presence of defects and it is used to determine the ratio of the D- and G-band intensities (I_D and I_G) for a qualitative analysis of defects) [209]. In extreme cases, the graphene layers of CNTs can be completely destroyed and the CNT are converted into amorphous nanoparticles. The localized damage to CNT deteriorates both the electrical and mechanical properties of the CNT/polymer composites [181].

3.2.2 Calendering

The calendar, also known as three roll mills, is an equipment that employs shear stresses created by rolls to mix, disperse or homogenize viscous materials. A calendaring machine consists of three adjacent cylindrical rolls (i.e., the feeding and the apron rolls rotate in the same direction, whereas the centre roll rotates in the opposite) running at different velocities (the mismatch between the angular velocity of adjacent rolls is typically ω1: ω2: ω3 = 1:3:9) [181, 210]. The narrow gaps (controllable up to 5 µm) between the rolls, combined with the mismatch in angular velocity, result in locally high shear forces with a reduced residence time. Through the gradually decrease of the gap between the rolls, along with the repeated passage of the material on the rolls, it is possible to achieve a controllable and narrow size distribution of particles in the matrix [182, 209]. The use of three rolls mill have been widely reported in the literature for CNT [210-214], CNF [215], multilayers graphene/ GO/ rGO [178, 216-219].

Pras et *al.* [220] prepared nanocomposites modified with 0.7 wt.% CNT using an intensive mechanical mixer and a three rolls mill. Qualitative dispersion analysis showed that the CNT dispersion degree increased (based on individual CNT) from 10 to 45 % between 5 and 240 hours of intensive mixing, while the percentage of micron-size agglomerates decreased from 37 to 13 %, respectively. Better results were obtained using the three rolls mill, with a dispersion degree around 75 % and only 2 % of micron-sized agglomerates. Campo et *al.* [221] used a calendaring process to disperse different types (long, short and amine functionalized) and loadings (between 0.1 and 0.5 wt. %) of MWCNT into an epoxy matrix. The dispersion cycle was composed by 4 stages where the gap between the rolls was continuously reduced from 120/40 µm (1st stage) to 15/5 µm (4th stage) at a velocity of 250 rpm. Based on the results obtained, this approach was successful to provide good dispersing of the different types of CNT in the nanocomposite. Moreover, Araujo et *al.* [178] studied the influence of the residence time and hydrodynamic shear stresses on the dispersion of different types of graphene particles (multilayers graphene and rGO) in an epoxy matrix, using a three rolls mill. The results evidenced that higher residence time and shear stresses promoted the reduction of size and number of agglomerates of samples prepared with 0.7 wt. % nanoparticles. Interestingly, Li et *al.* [94, 205] reported the direct *in-situ* exfoliation/dispersion of graphene in epoxy using three rolls mill without the need of any additives, solvents, compatibilizers or chemical treatments. Nanocomposites presented increased electrical conductivity for 1 wt. % loading.

On the other hand, Chandrasekaran et *al.* [216] compared the properties of multilayers graphene/epoxy nanocomposites prepared using different dispersion methodologies. Electrical and mechanical results denoted better dispersion achieved using the three rolls mill when compared with ultrasonication. Similarly, Imran and Shivakumar [222] evaluated the use of mechanical mixing, sonication and three roll mill on the properties of graphene/epoxy nanocomposites, denoting better results with the latter method. While other authors successfully combined ultrasonication with calendering to prepare epoxy nanocomposites with different loadings of multilayer graphene [223-226] and CNF [227].

3.2.3 Functionalization

According to the literature, the functionalization of carbon-based nanoparticles can be grouped into two main categories: i) chemical or covalent functionalization (new chemical groups are chemically bonded to the carbon atoms) or ii) physical or non-covalent (various molecules are physically wrapped around the nanoparticles).

Among the different types of chemical functionalization of CNM, wet functionalization *via* acidic oxidation is one of the most commonly adopted. It serves the dual goal of introducing new chemical groups and removing metal particles (trapped catalyst) and amorphous carbon. This is especially true when nitric acid (HNO_3) is used to remove residual metals and to introduce oxygen-containing groups (mainly carboxylic acid). Specifically, the acid treatment is to create covalent sidewall groups by an oxidative process with strong acids, such as HNO_3, sulfuric acid (H_2SO_4) or a mixture of them. For example, after this type of treatment, the hydrophobic surface of CNT turns into hydrophilic, which can be easily soluble and disperse uniformly in many solvents and polymer matrices, resulting in notably improved mechanical and other multifunctional properties for the bulk nanocomposite [228-230]. As mentioned in the previous section, GO is normally obtained from the exhaustive oxidation and exfoliation of graphite, and contains a range of oxygen functional groups with specific chemistry [105, 231, 232].

Tiwari et *al.* [233] carried out a quantitatively assessment on the dispersion quality of as-grown, oxidized, and functionalized CNTs in an epoxy matrix. It is shown that carboxylic functionalization reduces the average CNT agglomerate size and thus ensures better dispersion of CNT in epoxy at loadings between 0.05 and 0.25 wt. %. The improved dispersion leads to enhanced interfacial interaction at the CNT/epoxy interface and hence provides higher relative improvement in nanocomposite properties, such as tensile strength and modulus, compared to the samples prepared using as-grown and oxidized CNT. Yang et *al.* [212] evaluated the influence of the dispersion and interface on the mechanical properties of as received and functionalized CNT with COOH, using a three rolls mill. SEM and STEM observations denoted a better dispersion state of the functionalized CNT, which was further confirmed by the improvements on the tensile properties of the nanocomposites for a range of concentrations between 0.2 and 1.0 wt. %.

CNT containing COOH groups can be even further functionalized to introduce, for instance, amine groups able to confer improvements on the mechanical and thermal properties of the modified nanocomposites when compared to pristine CNT [234-236]. Mostovoy et *al.* [237] prepared epoxy nanocomposites containing pristine and amino functionalized MWCNT. Promoted by better particles' dispersion, the nanocomposites containing amine functionalized MWCNT presented tensile strength enhancement of 108 % and impact strength 300 % higher than the unmodified matrix, while the increase observed for pristine MWCNTs was 89 % and 225 %, respectively. In addition, Armstrong et *al.* [238] functionalized CNTs with different amine compounds that are commercially available as cross-linking agents for the epoxy resin, resulting in nanocomposites with improved mechanical properties. Moreover, Zhu et *al.* [239] introduced functional amine terminated groups *via* silanization to de surface of CNF to improve its dispersion in the epoxy matrix. Abdalla et *al.* [240] compared the properties of nanocomposites containing carboxyl and fluorine functionalized MWCNTs, denoting better dispersion in the matrix of the latter. Konnola and Joseph [241] proposed a new surface-modified of MWCNT with carboxyl terminated poly(acrylonitrile-co-butadiene) (CTBN) by side-wall functionalisation. Nanocomposites produced with 0.3 wt. % of this functionalized MWCNTs presented an improvement of ~117 % in fracture toughness and 25 % enhancement in tensile strength when compared to the neat epoxy, while the improvements were less significative for the nonfunctionalized MWCNT. While Park et *al.* [242] functionalized GO with amine terminated poly(acrylonitrile-co-butadiene) to improve the

dispersion of the graphene sheets in the matrix. The produced nanocomposites presented 50 % fracture toughness increase with 0.04 wt. % functionalized GO loading.

Ozone treatment of MWCNT is considered to have high efficiency, low cost, as well as easy operation, while also being able to operate at room temperature (RT) without the aid of organic solvents [243]. This treatment has also been employed to prepare CNT for further silane functionalization, to improve the dispersion of the particles in the matrix and the mechanical properties of the nanocomposite [244]. Silane coupling agents were also used by Kim et *al.* [245] to modified the surface of multilayers graphene to enhance the dispersion of the particles in the epoxy matrix. Alternatively, plasma treatment is another possible method for adding functional groups to CNT and improve their compatibility with the matrix. This approach is advantageous compared to acid treatments as it is a dry process and functionalisation can be done in one step. However, most of the reported investigations were performed on small scale, with typical quantities around 1 g at a time [246]. Williams et *al.* [247] developed an enhanced oxygen plasma treatment for 25 g of nanomaterials and scalable up to 1 kg, showing the presence of 3 wt. % of carboxylic acid groups and an increase in the bulk density from 151 to 76 $kg \cdot m^{-3}$, when compared to the as-received CNT.

Wan et *al.* [248] also reported the functionalization of GO with diglycidyl ether of bisphenol-A (epoxy groups), resulting in modified nanocomposites with improved tensile properties when compared to the neat epoxy and modified resin with "pristine" GO. And Yao et *al.* [249] produced enhanced nanocomposites using GO functionalized with 4-nitrobenzenediazonium salt, with tensile strength increase of 30 % and thermal conductivity 2.5 times higher than the neat epoxy.

On the other hand, non-covalent functionalization is based on the physical interaction between the nanoparticles and other chemicals, such as electrostatic interactions, van der Waals forces, hydrogen bonding, or π-π stacking interactions. Different types of polymers or block copolymers (for instance presenting one block with affinity with the nanoparticles and the other with the matrix) are able to create a layer surrounding the CNM, improving its dispersion and stability, avoiding re-agglomeration. Similarly, is it also common to use amphiphilic species, such as non-ionic surfactants (Triton X-100), anionic surfactants (sodium dodecyl sulphate, SDS), and cationic surfactants (cetyl trimethylammonium bromide, CTAB).

This methodology, when compared to the chemical functionalization, presents as an advantage the fact that the structure of the CNM is not damaged [181]. However, the efficiency of the particles dispersion strongly depends on the nature of the polymer/surfactant and the amount of dispersant used. In fact, excessive levels of dispersant may have a negative impact on the mechanical, electrical and thermal properties of the modified composites, despite providing good particle dispersion [250]. The total wrap of the particles with the dispersing agents may prevent particle-particle interactions needed for the formation of conductive networks throughout the matrices [251].

Jaemin Cha et *al.* [252] produced nanocomposites containing poly(styrene sulfonate) (PSS) and poly(4-aminostyrene) (PAS) attached on the surface of CNT by noncovalent functionalization. At first, stable noncovalent functionalized CNT/solvent dispersions were achieved when compared to the pristine CNT. The mechanical performance of the modified nanocomposites was improved, in particular for the materials containing 1 wt. % of PAS-CNT. Moreover, Loos et *al.* [253] studied the use of 8 different dispersing agents, polymers and surfactants, on the properties of nanocomposites containing 0.075 wt.% MWCNT. Even though the addition of these agents resulted in stable epoxy suspensions, only a few resulted in nanocomposites with improved tensile properties (L-7602 and BYK-9077). Geng et *al.* [254] demonstrated the successful use of Triton X-100 to disperse CNT, with improvements in flexural properties and electrical conductivity. While Wan et *al.* [255] used the same surfactant to disperse rGO and prepare modified nanocomposites with improved tensile properties with loadings bellow 0.2 wt. %. Similarly, Poutrel et *al.* [250] reported the successful use of Triton X-100 to disperse multilayers

graphene, denoting electrical and thermal improvements (up to 220 % increase in thermal diffusivity at 5 wt. %).

Apart from the most common methods previously mentioned, a few authors also reported alternative approaches. Hameed et *al.* [256] reported the combination of ultrasonication with the use of ionic liquids (IL), since it is proposed that the π– π stacking interactions of CNT are shielded by the high dielectric constants of IL restricting them from rebounding. In this case, the IL 1-butyl-3-methylimidazolium tetrafluoroborate ($BMIMBF_4$), was used both as a dispersing agent and a curing initiator for the epoxy resin, becoming part of the crosslinked matrix. Reinforced nanocomposites with 0.7 wt.% of MWCNT presented a 95 % increase of the plain-strain fracture toughness (K_{IC}) when compared to the neat epoxy. Recently, Naeem et *al.* [257] developed a facile, green and novel approach has the for preparation of well dispersed graphene/epoxy nanocomposites, involving microwaving of a commercial graphene precursor and mechanically stirring to produce multilayers graphene in a hot, liquid-state epoxy resin, eliminating the need for organic solvents and surfactants.

Based on the literature, Table 4 presents a summary of the advantages and disadvantages of the main dispersion techniques normally used to disperse CNMs.

Table 4 Resume of advantages and disadvantages of each dispersion methods [181, 182, 209].

Dispersion Method	Advantages	Disadvantages
Ultrasonication	Good level of dispersion achieved.	Risk of damaging the structure of the CNMs. Use of solvents (not environmentally friendly, and additional steps for its removal). Causes heat of the solution. Not very appellative from an industrial point of view.
Calendering	CNMs can be directly dispersed in the polymeric matrix. Great dispersion achieved. Scalable method.	It may require multiple cycles and long time to achieve good particle dispersion. Aggressive conditions may result in damages on the CNMs.
Intensive mixing	CNMs can be directly dispersed in the polymeric matrix. Scalable method.	So far, limited levels of dispersion achieved.
Chemical functionalization	Improved compatibility with the matrix and good dispersion achieved, in particular when used in combination with other dispersion techniques.	Introduction of damages on the CNMs. Reduction of the electrical properties of the particles. Not environmentally friendly. Some methodologies are not scalable.
Physical functionalization	Improved compatibility with the matrix and good dispersion achieved, in particular when used in combination with other dispersion techniques. Does not introduce damages to the CNMs. Scalable method.	Large quantities may be required to achieve good dispersion, which can also lead to a decrease of the electrical conductivity of the composites.

3.3 Carbon fibre reinforced polymer composites

As previously mentioned, thermoset resins are commonly used for the preparation of high performance CFRP for demanding applications. Besides the improvement of mechanical properties, the introduction of CNM has the advantage of providing other attributes to the modified material (multifunctionalities).

Recently, increasing interest is found on the production of CFRP with self-sensing abilities as a way of structural health monitoring (SHM), based on changes of the electrical conductivity of the materials. The ability to detect and monitor the internal damage state of a CFRP structural part would introduce huge advantages, for instance in the aerospace sector, since nowadays the parts are typically overdesigned to offset the possibility of unexpected internal failures, which works against the weight reduction purpose of using them in the first place [258]. This feature would also allow the set-up of proper safety thresholds and the risk reduction of catastrophic failures. The first self-sensing concept for CFRPs relies on electrical methods to detect the internal health status of composites using the intrinsically conductive CFs as damage sensors. Nevertheless, due to the highly anisotropic conductivities of CFs, the failure modes that can be self-sensed are mostly fibre breakage, which normally occurs near the end of a component service life. Since early stage damage and matrix failure modes, cracking or delamination, depend strongly on the resin (typically insulating), different CNMs have been introduced to increase the matrix electrical properties [258].

Focussing on CFRPs based on continuous carbon fibre or fabric surrounded by a polymeric matrix, there are several manufacturing technologies available and hand layup, prepreg combined with autoclave, vacuum infusion, pultrusion and filament winding are considered the most relevant [259]. There are also interesting automated approaches already used in certain industries, which allow the increase of production throughput, including additive manufacturing, automated fibre or tape placement or combinations between complementary technologies [259-261]. Regarding the development and production of modified thermoset based CFRP, there are two main approaches to utilize CNMs which can be mainly divided into: 1) matrix modification and 2) fibre modification (Figure 4).

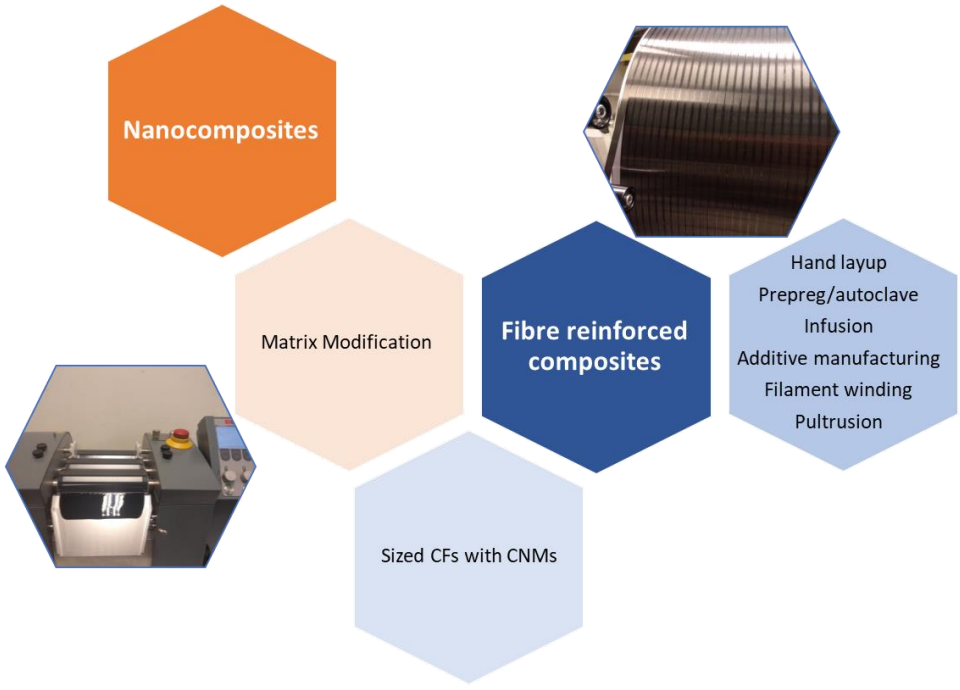

Figure 4 Main approaches to manufacture modified CFRP with CNM.

3.3.1 Matrix modification

In general, the previously reported methods for the successful dispersion of CNM in the epoxy resin are applied to further produce multifunctional CFRPs. Based on the literature, the most common production methods using modified resins are hand layup, pre-impregnation and infusion. It should be noted that the simplistic term “infusion” here used embodies a wide variety of methodologies, such as resin

transfer moulding (RTM), vacuum assisted resin transfer moulding (VARTM), or vacuum assisted resin infusion (VARI), among others [262].

In the past years, the utilization of CNM to reinforce and introduce multifunctionalities in CFRPs has been extensive. However, the electrical or mechanical improvements are not always observed or linearly passed from nanocomposite to fibre reinforced composite level. The addition of CNM into the resin can introduce complexities related to increased viscosity, CNM filtration, uneven coating throughout the laminate, improper bonding between the layers and penetration of resin into the fibres [262]. Also, the CFRP manufacturing procedure plays a significant role on the final properties of the modified materials. For instance, Abdelal et *al.* [263] used modified resin with 1 and 2 wt.% CNT to produced nano-enabled CFRP by hand layup assisted with vacuum bagging. In general, the tensile properties of the modified composite materials were similar to the reference. While Hsiao et *al.* [264] reported the preparation of CFRP using a similar methodology and modified matrix with 0.3 wt. % of CNF. The CNFs were aligned transverse to the CF fabric (z-thread), which resulted in a 29% increase of the interlaminar fracture toughness (G_{IC}). Using the same methodology, Kandare et *al.* [265] explored the influence of GNP on the through-thickness electrical conductivity of CFRPs by measuring the laminate electrical volume resistivity. 55% reduction in the through-thickness electrical volume resistivity was achieved with an addition of 1 vol. % GNPs. Even tough hand lamination is a simple and well-established fabrication method, it is normally not compatible for industrial scale, in particular for high demanding applications.

Regarding the pre-impregnation process, Santos et *al.* [266] produced unidirectional (UD) prepreg materials and CFRP containing 0.043 wt. % of pristine or functionalized MWCNT, which resulted in interlaminar fracture toughness increases of 11 and 44 %, respectively. These findings denote impressive enhancements at ultralow particles loading can be achieved if a homogeneous and stable dispersion is ensured as well as a stronger interfacial bonding. Godara et *al.* [267] also produced prepreg materials modified with 0.5 wt. % of pristine and functionalized CNT, obtaining an interlaminar fracture toughness increase of 80 %. Kostagiannakopoulou et *al.* [268] used the same methodology to prepare UD-CFRPs containing modified resin with 0.5 wt. % GO and GNPs, denoting similar interlaminar fracture toughness improvements around 50 % for both particles. Araujo et al. [178] obtained both interlaminar fracture toughness and transverse electrical conductivity improvements on modified CFRPs containing 0.09 wt. % of rGO and 2.1 wt. % GNP. While impressive 227 % transverse electrical conductivity increase was obtained by Rodríguez-García et *al.* [269] for CFRPs containing 2 wt. % GNP.

Researchers have also extensively used infusion approaches to prepared modified CFRPs including the matrix modification with CNT [270], CNF [271], GNP [272] and graphene GO [273]. However, some of these studies highlighted potential manufacturing issues regarding the use of modified matrices with CNM, not only due to its increased viscosity that further difficult the infusion process, but also because ofnanoparticles filtration by the CF fabric that results in a non-homogeneous distribution. In these cases, the agglomerates of the CNM can act as defects and decrease the overall mechanical performance of the final material, without contributing to the improve to the transverse electrical conductivity [274].

In addition, Qin et *al.* [275] showed that the introduction of GNP in CFRPs could bring an increase of 165% in the electrical conductivity through the thickness direction, compared to those without GNP, generated by a continuous conductive path between CF and epoxy from one side to another in composite. The electrical conductivity through the thickness was greatly enhanced because of the ability of conductive GNP to percolate with each other and to connect adjacent CF.

3.3.2 Fibre modification

Another interesting way to introduce CNM in multiscale CFRPs consist in the modification of the CFs with the nanoparticles, as represented in Figure 5. This can be done using different surface treatment methodologies, such as electrophoretic deposition of CNF [276] or GO [277], spraying of GNP solutions [278], sizing with CNMs solutions [279], or even *in situ* growth of CNT on the CFs [280].

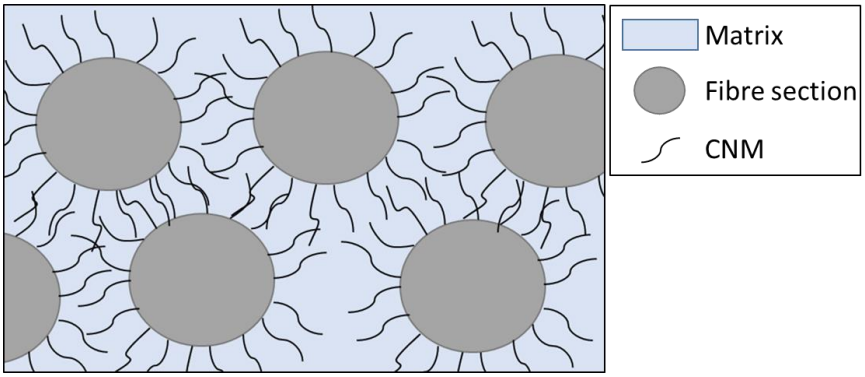

Figure 5 Illustration of the reinforcement from the modified fibres with CNT in the hybrid composites.

Boroujeni et *al.* [281] developed CFRP by hand layup assisted with vacuum bagging and hot press, with CNT grown on the CF (varying several parameters on the CNTs growth). The tensile results obtained for the different modified materials were similar to the reference, with only 11 % increase of the tensile strength for the samples where the underlying nickel catalyst formed a fine checkerboard patterned and the fabric coated with 75 mm silicone dioxide (SiO_2) and 2 mm nickel catalyst films, where the CNTs were grown thereafter. Islam et *al.* [282] used a chemical method to graft CNT onto CFs by direct covalent bonding to form a CNT-CF hierarchical reinforcing structure, *via* ester linkage (formed at 70 °C without using any contaminating catalyst or coupling agent). The modified CFRP presented increased electrochemical capacitance properties by rapid ion diffusion through active CNT sites and defects created during grafting (specific capacitance 3.5 times greater than pristine CF), indicating substantial promise as a material for fabricating textile supercapacitors with superior strength, flexibility and performance.

Li et *al.* [283] prepared aqueous suspension with commercially functionalized CNT that were further used to coat CFs. Depending on the type of commercial CF, CFRPs containing COOH-CNTs presented interfacial shear strength increases of 43 and 12 %. Similarly, Zhang and co-workers [279] prepared CFRPs with modified CFs with sizing solutions containing different loadings (1 to 10 wt. %) of CNFs. After the push-out tests, it was found the CFs sizing with CNFs could generally increase the interfacial shear strength, in particularly for lower nanoparticle addition.

CFRPs with improved damage sensing capabilities were developed by Zhang et *al.* [284] through the application of low concentrations of CNT into CF prepregs using a spray coating technique. Besides interlaminar fracture toughness enhancements of 50 % with 0.047 wt. % CNTs addition, excellent sensing signals were obtained and analysed, with good correlation between crack propagation and electrical resistivity.

4 Thermoplastic-based composites

Thermoplastic polymers are widely used as matrices for composites with CNM [285-290]. Their main advantage is the possibility to use melt processing for the composite production and shaping methods which can be easily scaled up by available extrusion and injection moulding methods. Many thermoplastics can also be dissolved in common solvents and thus, composites can be further manufactured by solution mixing and shaping from such dispersions. In principle, all thermoplastic polymers can be processed in such CNM containing composites. Other preparation methods applied to thermoplastic-based nanocomposites are the in-situ polymerisation in presence of nanofillers (in melt or solution) [291, 292] and the latex approach [293, 294]. Other shaping methods of thermoplastic-based CNM containing composites are compression moulding, shape extrusion (e.g., tubes, profiles), melt or solution spinning [295-297], foaming [298-300] and 3D printing [301, 302].

Based on the intrinsic properties of CNMs themselves, as described above, mainly the unique property of being electrically conductive is exploited in conductive polymer composites (CPCs) for many applications, such as antistatic housings, electromagnetic shields, conductive electronic parts, etc. For this, the filler amount added has to be above the electrical percolation threshold, ϕ_c, which means that the conductive filler has to form a pathway that goes through the matrix and thus, makes the whole material electrically conductive. However, the nanofiller do not have to contact each other directly, as the electrons are able to tunnel hop over certain distances (assumed to be in the range below 10 nm). Thereby, the aspect ratio of the filler plays an important role, with the general trend being that the higher the aspect ratio, the lower the electrical percolation threshold.

However, also the excellent mechanical strength of CNM is a reason to incorporate them in thermoplastic matrices and to make the corresponding polymer matrices stiffer, stronger [289], better scratch resistant, less breakable, with lower creep behaviour [303, 304] etc. The effects are usually higher the greater the difference between the moduli or the mechanical properties of the matrix and the filler, which means that higher effects can be achieved in softer materials. The filler amount dependence is often not linear, as at higher loadings remaining primary agglomerates reduce the available surface of the nanofillers for interfacial adhesion or act as starting points for cracks. In addition, at the filler content when an electrical network is formed, typically the elongation at break reduces significantly as the typical deformation behaviour of the matrix is disturbed by the network [305].

In addition, the crystallization behaviour of partially crystalline thermoplastics can be influenced as CNMs with their high surface area act nucleating [306] and can reduce e.g., cycle times in injection moulding. Also, the fire behaviour may be positively influenced, e.g., by reducing the maximum heat release rate or reducing the induction time [307, 308]. Barrier properties can also be improved, especially when platelet-like fillers (such as graphene or graphene and graphite nanoplatelets) are used [309, 310]. The thermal conductivity typically is also improved, even if much higher contents than for electrical conductivity are needed to see significant changes due to the needed phonon transport requiring nearly direct filler contact [311-313].

Another property which derives from the electrically conductive character of CPCs are their ability for sensing [314], such as deformation or strain sensing [315, 316], liquid sensing [296, 317], vapour sensing [318] or temperature sensing [319]. The sensing ability derive from changes in the electrically conductive network structure when the composite or polymer matrix is exposed to strain or temperature changes or is swollen by solvents with suitable polymer interactions or their vapours. The sensing behaviour is then assigned to changes in the electrical resistance of the composites upon exposure.

Based on mainly the electrical properties, also the EMI shielding behaviour of polymers can be dramatically improved when adding CNM [320]. This enables applications to protect critical electrical

devices and to save the environment from harmful electromagnetic waves. Next to that, CPCs also can show thermoelectric properties, meaning that temperature differences at the surfaces of such composites can be transformed into an electrical thermovoltage [321, 322].

In this sense, CNM can be regarded as multifunctional additives also in thermoplastics.

4.1 Main drawbacks when using CNM in thermoplastics

The effects of CNM in matrices strongly depend on the degree of CNM dispersion and the interfacial adhesion. As most CNM are produced in an agglomerated state [323-325], the break-up of such agglomerates and the individualization of the primary particles is essential. How good such dispersion is possible depends on the structure and the agglomerate strength of the primary agglomerates. For the example of MWCNT, bird-nest structures or yarn-like structures are reported which have different dispersibility [326]. It was found that higher shear stresses are needed to individualize agglomerates of the material Baytube C150P as compared to those based on Nanocyl NC 7000 [326]. There are several processes involved in the dispersion of primary agglomerates, which are the infiltration and wetting processes of polymer melts inside such primary agglomerates followed by the break-up or erosion of the agglomerates and the subsequent distribution of the smaller agglomerates or primary particles in the matrix [327]. As polymer melts are compared to epoxy resins much more viscous, the infiltration step is typically worse. A good infiltration process would require loose agglomerates and long time and would be as better as lower the viscosity of the matrix is [328]. Another factor which plays a role for infiltration and wetting is the interfacial tension between the matrix and the filler: higher interfacial tension is commonly associated with worse wetting ability and interfacial adhesion between matrix and filler. For example, depending on the surface tension of different polymers and one type of MWCNT, larger primary agglomerates were found at higher interfacial tension [328]. For the second step of the dispersion mechanisms, the break-up and erosion processes, the relatively high viscosity of polymer melts is favourable. Higher shear stresses typically lead to better dispersion, meaning smaller remaining agglomerates or even complete individualization. The process of distribution is also favoured by thermoplastic melts; sedimentation processes that occur for epoxy matrices typically do not take place.

Even if quite a high amount of research was spent into the topics of dispersion and enhancing interfacial interactions, these two problems are still a drawback when looking towards industrial applications.

4.2 Strategies to maximize the properties of the CNM based composites

4.2.1 Enhancing interfacial interactions between CNM and thermoplastics

In order to improve the compatibility between the polymer matrix and the CNM filler, the interfacial tension between both should be low. For a given polymer/CNM combination, this can be achieved either by modification of the CNM' surfaces, e.g., by adding functional or even reactive groups during the synthesis or covering with additives bearing functional groups or by modification of the polymer matrix. In addition, additives, often called as compatibilizers, can be added which typically have parts which are compatible with the filler and compatible with the matrix. Such additives also can induce chemical reactions to the composite components.

For polypropylene (PP), a typical modification is the anhydride grafting of the matrix or part of it. The maleic anhydride groups show high interaction, sometimes even reactions, with the functional groups existent at the surface of most CNM, such as -COOH or -OH groups. For example, it is reported in the literature that a styrene maleic anhydride copolymer was applied to enhance the dispersion of CNMs in

polyamide 12 [329, 330]. Another example is the use of peroxide in order to create reactions between CNTs and the polymer matrix, as described in for PP-MWCNT composites produced using a laboratory scale extruder [331].

4.2.2 Enhancing dispersion of CNM in thermoplastics

The processing conditions also play an important role on the achieved state of dispersion [305, 328, 332-334]. Taking twin-screw extrusion as an example, it was found for the dispersion of pristine MWCNTs that the following parameters influence the state of CNM dispersion:

Screw configuration: The screw length and the order and geometry of the used mixing and conveying elements play an important role on the dispersion of primary agglomerates and thus, on the resulting properties. There are only few systematic studies reported on this issue, which concern polycaprolactone (PCL) and polycarbonate (PC) based MWCNT composites. In general, the use of back-conveying elements and the extension of the processing length resulted in an increase in the residence time which is favourable for the nanotube dispersion. When using distributive screw configurations containing mixing and conveying elements the CNT dispersion can be enhanced as compared to dispersive screw configurations with kneading and conveying elements in the metering zone [335, 336].

Nanofiller feeding position: Depending on the structure of the carbon nanofiller material, feeding with the polymer in the hopper or feeding in a side feeder in the already molten polymer may be favourable for a suitable dispersion and good electrical and mechanical properties. This was shown for example for different types of MWCNTs when incorporated into polypropylene (PP) [337]. The recommendation was that the more compact Baytubes C150P agglomerates should be added into the hopper, whereas for the more loosely packed Nanocyl™ NC7000 agglomerates, addition using the side feeder resulted in better dispersion, lower electrical resistivity, and higher mechanical properties.

Incorporation of the nanofiller by direct incorporation or using a masterbatch: In general, it is found, that the two-step extrusion when preparing a masterbatch with high filler content in the first step and then diluting it to the desired concentrations results in better nanofiller dispersion than the direct incorporation. However, on the other hand one has to consider that the specific mechanical energy (SME) introduced by the two-step procedure is higher and that, in addition with the second melting step, the reduction in particle sizes may be higher. For the example of MWCNTs in PP, it was shown that the electrical resistivity of composites produced using the masterbatch approach was higher than that direct incorporation, even if the dispersion was better. This indicated that a more pronounced MWCNT shortening occurred in the two-step procedure [338].

Throughput, rotation speed, melt temperature: There are some studies which systematically investigate the influence of these factors. One has to consider that the input of SME as well as the residence time are dependent on these conditions and are varied when changing those. Thus, clear tendencies are difficult to obtain. In general, it was found that both, an increase in rotation speed and throughput resulted in a decrease of the residence time. The increase of rotation speed led to higher SME inputs inducing a significant better CNT dispersion, whereas an increase in throughput resulted in worse dispersion [333, 335, 339-341]. These influencing factors are also found and discussed in the literature for the dispersion of GNPs in PP [342, 343].

In addition, the use of unconventional methods, such as introducing ultrasound in the extruder is reported to enhance the dispersion and by such the properties of CNM containing composites [344-347].

In all these variations of processing conditions it should be also considered that harsh conditions can affect the size and aspect ratio of the CNM fillers in a negative way. For example, Krause et al. [323, 348] found, that after melt extrusion in a twin-screw extruder the initial length of MWCNTs (here Nanocyl NC 7000) was reduced to about one third. This reduction was not only strongly dependent on the

extrusion conditions, but also on the CNT concentration in the composites [349]. For expanded graphite nanoparticles, extended mixing time (in small-scale mixing) resulted next to a better macrodispersion in a reduction in lateral size which could explain the increase in electrical resistivity with mixing time [342].

As second main strategy, the use of additives supporting good dispersion of CNMs is widely studied. Such additives help in different ways. If premixed with the filler, they reduce the agglomerate strength of the primary CNM particles due to their typically low viscosity and good penetration in the agglomerate structures. During mixing they stabilize dispersed particles in the melt due to their localization at the interface between filler and matrix and prevent the often-observed process of secondary agglomeration. Examples are given by Müller et *al.* [350] when using PEG in polyethylene (PE) based MWCNT composites. PE has low interactions with MWCNT, however when using PEG a significant increase in the state of dispersion (observed from light microscopy images and SEM studies) could be found. Similar to what was stated previously for the thermoset-based composites, IL can also be used to enhance the dispersion of CNT. Socher et *al.* [351] reported significant dispersion improvements for PA12/MWCNT composites using imidazolium based IL. Bifunctional coupling agents were also reported to reduce the percolation threshold of MWCNT in PA12 by a factor of 3 [352].

4.2.3 Adapting the CNM content to find the optimum for the desired application

Typically, the properties of CNM based composites increase with the filler loading [353-366]. For electrical properties, the percolation threshold characterizes the concentration where a trough going filler path is formed and at which the electrical conductivity increases dramatically by many decades. It is known that a good adhesion between filler and matrix interphase plays crucial role to properties of the reinforced polymer composites [367]. For mechanical properties, the modulus typically increases nearly linear at low loadings, but not in the same intensity at higher loadings. This is ascribed in the literature to the increasing difficulties to disperse the CNM adequately at higher filler loading. In addition, the crystallinity of the CNM-composites varied depending on CNM loading and resulted a change on the modulus. Qiu et *al.* [366] concluded that the molecular chains in the PP matrix can move easily due to CNMs acting like a lubricant at the certain loading. It is known to reduce the crystallinity and *Tc* of waxy materials when added in high doses, and therefore it is seen a decrease in modulus of the reinforced thermoplastic composites. Impact strength frequently increases or reaches a maximum as a function of filler content into thermoplastic polymer matrix.

It has been reported in studies that nano-sized carbon fillers such as CNT increase mechanical properties and electrical conductivity more than other carbon fillers, especially at low loadings [354]. According to Vilaverde et *al.* [368] investigated the conductivity of nanocomposites made of 2 and 10 wt. % GNP loading, and concluded that even at high loading, the presence of a network of well-dispersed particles and aggregates is important to increase conductivity. On the other hand, for superior mechanical properties in nanocomposites, it is essential that the CNT or the other CNM are uniformly dispersed into the polymer matrix. Santos et *al.* [342] studied the effect of particle size (range between 2 and 15 nm) of GNP on the dispersion and electrical conductivity properties of GNP/PP composites. The agglomerate area ratio (A_r)increased for three different type of GNP in the PP matrix when provided a flow at a sufficient low shear rate and time. Other authors reported that the tensile strength values decreased when CNT loading was 1.5 wt. % in the polymer matrix [369, 370].

On the contrary, researchers have been encountered some difficulties at high loading of CNT. The main difficulties while producing CNT based composites are inadequate dispersion effect due to the high surface areas (aspect ratio: >1000) [182], and weak adhesion interface between nanoparticles and polymer matrix. As previously mentioned in other sections, it has been proven that surface modification

or functionalization of CNM promotes adequate distribution and mobility of the molecular chain in the polymer matrix [371]. Shanmugam and co-workers [367] revealed that 0.03 wt. % of CNT by modifying the surface with dopamine caused an improvement by 42.3 % in tensile strength by enhancing adhesion of filler/thermoplastic matrix interphase.

Machinability of CNT reinforced plastic composites with three filler loading as 1.75, 5 and 15 wt.% was studied by Samuel et *al.* [372]. This study reported that visco-elastic/plastic deformation of the polymer-phase was important with low amount CNT loadings (1.75 wt. %), whilst over 5 wt. % filler loading, CNT distribution and interface effects governed the machinability of the composite. They concluded that the machinability and thermal conductivity of the composite enhanced with the increase CNT loading.

As it can be seen, many factors affect the properties of CNM-based composites, but three factors must be also considered: performance, cost and minimum environmental hazards. It should be reached an optimum equilibrium between them. Artificial intelligence techniques are the easiest and cheapest way to design composites and predicted desired properties. Ozturk et al. [373] investigated a new approach by using particle swarm optimisation (PSO) technique in the production hybrid thermoplastic composites. The determination of optimum content for each component of the CNM composites created in simulation environment. In their studies, they focused on reducing the cost of composites and accelerating the production process, and achieved a success rate of over 90 % in the tensile properties of the hybrid thermoplastic composites produced according to the best formulation obtained with PSO optimization. It is thought that this technic could be applied on determining of optimum CNM filler(s) ratio of the nanocomposites for a desired application.

5 Other applications of CNM

Apart from the previously mentioned utilization of CNMs to produce composites materials, both thermoset- and thermoplastic-based, there are also other applications of these particles that have been explored int eh past years.

5.1 Metal Organic Framework composites

Metal Organic Frameworks (MOFs) are solid porous materials classified by IUPAC on 2013 as a sub-class of Coordination Networks, which are a sub-class of Coordination Polymers with an open framework containing potential voids [73, 374]. They are characterized by three-dimensional structure, arising from strong coordination bonds between metal nodes (metal ions, metal centers, or metal clusters) and the organic linkers (organic molecules containing one or more N-donor or O-donor atoms like organic carboxylates, pyridyl derivatives, cyano compounds, polyamines, imidazole derivatives, oxalic acid, phosphonates, sulfonates, and crown ethers) [375, 376]. MOFs are synthetized mainly in the liquid phase by mixing solutions of precursors under solvo(hydro)thermal conditions at a high temperature and pressure. Alternative synthetic methods, including mechanochemical, electrochemical, microwave, and sonochemical slow evaporation methods have been proposed in recent years [375].

MOFs are promising and versatile materials for different technological applications, since they have been used as catalysts, absorbent for gases (including toxic gases) and metal ions and also find applications in biomedical sector, thanks to the biocompatibility of some formulations, as drug carriers, bioimaging agents and therapeutic agents [377, 378]. MOFs have been also used as materials for supercapacitor electrode preparation [379], as sensing layer in detection devices [380, 381] and as support for chromatographic analysis [382].

The most distinctive and attractive MOFs structural characteristics are high surface area, presence of open metal sites, open framework, tunable pore sizes and flexible porosity [375]. Unfortunately, along these promising physical and chemical properties, MOFs exhibit general low electrical conductivity, poor thermal, chemical and mechanical stability, instability in the presence of humidity or upon a solvent removal and weak gas retention capability because of weak dispersive forces that can limit gas sorption and storage capacities [383-385]. To ensure the potential use of MOFs in large-scale applications at high technology readiness level (TRL), most of these limitations must be addressed. To this aim, the production of new materials by compounding MOFs with other functional materials is gaining a lot of attentions [386-388].

The formation of hybrids/composites through the controllable integration of MOFs and functional materials, is expected to lead to new materials exhibiting properties that are superior to those of the individual components since they combine, in a synergistic way, the advantages of both parent materials. MOFs have been compounded with polymers [389], oxides [384], metal nanoparticles [390] and CNM [38, 133, 134, 391]. However, the mechanisms involved at the materials' interface are not completely understood so the characterization of these systems is still challenging. Moreover, the synthetic strategies have a relevant role in determining the final material morphology and homogeneity as well as its properties.

In principle MOF composites can be applied in every field where MOFs can be applied, with additional new possibilities in applications where pure MOFs cannot be exploited. MOF composites can be synthetized by different approaches as recently reviewed by different authors [387, 388]. The most used methods are: encapsulation, layer-by-layer deposition, and in situ growth. The first approach allows to trap the other component/components within the MOF pores, the second to cover the MOF with the other component/components and the third to grow MOFs crystals in situ with the other species [387].

MOF-based composites have been produced with a wide array of CNM: CNT [391], fullerenes [392], CD [38], graphite [393], graphene and graphene related materials (GRM), such as GO and rGO [134] . In particular, GRM account for a wide population of materials containing aromatic sp^2 domains and have gained a lot of interest as possible carbon-based components in MOF composites for their unique structure, low toxicity, excellent electronic, thermal, electrochemical, and mechanical properties. Thanks to the presence of heteroatoms containing functional groups and the aromatic sp^2 domains, GRM can act not only as structural entities, but also participate in bonding interactions, enhancing the coordination bonding and guide the growth of MOF, providing a more beneficial structure. Additionally, GRM are expected to improve the properties of the composites acting to increase available active sites, to enlarge specific surface area, to modify structure, improve conductivity and accelerate electron transfer. MOF/GRM composites integrate the advantages and mitigate the shortcomings of the individual components, enabling the composites to possess an overall improved stability, enhanced electrical conductivity, higher gas selectivity [134, 384].

As concerns the type of MOF selected for the production of MOF/CNM composites, the HKUST-1 (also known as MOF-199 or $Cu(BTC)_3$) is widely represented, being considered as a benchmark material [394]. Also, MOFs of MIL family, Zn-based MOFs (MOF-5 and ZIFs) as well as MOFs belonging to the UiO family have been compounded with CNM. In the end, other composites have been found with TMU-16-NH_2, MOF-235, Cu-BDC-NH_2 and MOF-505 and with MOFs based on transition metals MOFs [Co-MOFs and Ni-Co-MOF/GO] [134, 384, 395].

A wide variety of approaches have been developed and applied for the preparation of MOF/CNM composites. Up to now, the most common way to obtain MOF/CNM composites is based on the *in situ* growth approach: MOF crystals are allowed to grow under solvothermal/hydrothermal conditions in presence of small amounts of CNM [395]. Another strategy to form in-situ MOF/CNM composites consists in a covalent or non-covalent pre-anchoring step of the ligand onto the CNM surface [395]. This approach is mainly used with GRM, indeed, Jahan et *al.* [396] covalently functionalized GO with a benzoic acid derivative and they observed that such a functionalization strongly affects the structure of MOF-5 within the composite. Other studies described the non-covalent functionalization of GO by introducing MOF ligands possessing aromatic rings able to form with GO π-π interactions. Mechanochemical and sonochemical approaches have been proposed as well [393, 395, 397]. MOF/GRM composites have been synthetized also by microwave-hydrothermal method [398]; since the microwaves increase the reaction kinetics, MOF composites can be obtained in a very short time with low power consumption and in an environmentally safe framework. Different MOF/GRM composites have been also fabricated by implementing the electrophoretic deposition (EPD), a low-cost technique used to grow nanostructures on conductive surfaces. With this method, MOF crystallites are uniformly deposited atop graphene sheets. In addition, less common methods have been also proposed: Bian et *al.* [399] described the synthesis of $Cu_3(BTC)_2$/GO by pickering emulsion, while Szczesniak et *al.* [400] proposed a method in which MOF crystals were allowed to form in the void spaces of 3D graphene structure, leading the GRM to act as a host platform to accommodate the nucleation of the MOF crystals.

All the synthetic approaches above mentioned allow the MOF structure to be successfully synthesized in the presence of CNMs, indeed it was found that the resulting composites exhibit structural features similar to the parent MOF, but overall distinct properties. Nevertheless, due to binding competition between the heteroatoms containing groups on CNM surface and the oxygen atoms of the MOF ligand towards metal cations, the possibility of producing heterogeneous samples should be considered. This binding competition can also cause the density of MOF particles decorating the CNM surface to not be optimal, which might decrease the synergy effects between the MOF and GO and therefore the overall performances.

The presence of CNM in the synthetic medium even if it does not affect the MOF nucleation leading to an overall preserved crystallinity of the MOF materials, it apparently modifies the morphology of the crystals, indeed in most cases they exhibit small and irregular particles, a significant surface roughness and several defects [133, 134]. Depending on the structure of the MOF, the interactions between the metal nodes and the CNM can induce the formation of a new porosity (micro and/or mesoporosity, depending on the parent MOF) at the interface between the carbon layers and the MOF units. In most cases, the specific surface area values measured for the composites with different GRM contents were always higher than those calculated for the corresponding physical mixtures [133] confirming the interaction between the composite components and the instauration of a kind of synergisms between them. However, there are some reports that do not follow that trend and a lowering in both surface area and total pore volume was detected with the increase of GRM loading. In most cases, the composites featured better thermal stability in comparison to the pristine MOF [134]. The intercalation with GRM imparts also new electrical properties to the composite while the pristine MOF is usual insulating. Alfè et *al.* [133, 134] imbedded conductive GL into the structure of copper-based MOF trough a one-pot strategy improved the MOF conductive properties. They demonstrated that the presence of embedded GL layers induces a non-linear increase of the electrical conductivity up to 5 orders of magnitude when the GL amounts accounts to 40 wt.% in the composites (10^{-2} $S \cdot m^{-1}$). The peculiar MOF/GL electrical conductivity also pave the way for application in advanced technological fields as sensors development that are currently under study.

5.2 Coatings prepared by Matrix Assisted Pulsed Laser Evaporation technique

Matrix Assisted Pulsed Laser Evaporation (MAPLE) is a technique developed for the deposition of thin films in late 1990s at the U.S. Naval Research Laboratory (McGill, 2000]). It is particularly suited for organic molecules, polymers and biomolecules [401, 402], but it also allows for the fabrication of either inorganic, organic, or hybrid coatings with a high versatility. Recently MAPLE technique has been used in a purposely adapted configuration for the preparation of new concept GRM coatings [403].

MAPLE is based on the same principle of pulsed laser deposition (PLD), but it uses milder conditions to provide a gentler and less damaging deposition. This technical feature avoids organic material decomposition, degradation, and/or denaturation induced by high laser powers during ablation. As a consequence, safe transfer and deposition of delicate compounds such as proteins or biopolymers including polymer nanocapsules for light-induced release [404-412] is achieved with the preservation of functional characteristics and structural integrity.

The target of MAPLE is a frozen solution of the material to be deposited in a volatile and light absorbing solvent, able to absorb most of the laser radiation (e.g., toluene), avoiding or reducing the photo/thermo-chemical damage to the molecule to be deposited. Indeed, the major part of the laser energy is absorbed by the solvent molecules and not by the fragile solute [401, 402, 413]. During the deposition process, the laser beam, overheating a small area of the target up to the limit of its thermodynamic stability, favors the ejection of a mixture of liquid droplets and gas-phase matrix molecules. The solvent is pumped away by a vacuum system and the solute molecules/particles impact onto a receiving substrate, typically placed parallel with respect to the target and at a fixed distance, generating a thin coating with thicknesses from a few to several hundreds of nanometers. The most employed laser sources are UV laser beam, IR laser beam and excimer lasers. Compared to other conventional, non-laser deposition methods (e.g., drop-casting, spin-coating, dip-coating, Langmuir–Blodgett), the MAPLE technique allows for high experimental versatility and high control of coating thickness allowing ultrathin film production of delicate molecules/particles [404, 412].

Since the solvent is pumped away by a vacuum system, MAPLE is a dry technique: thanks to this peculiarity, MAPLE technique provides enhanced molecules/particles adhesion to any substrate compared to wet techniques. In addition, MAPLE is compatible with masking, allowing to obtain finely patterned nanostructures.

The film deposited via MAPLE typically exhibit rough surface with large or small clusters. The rough surface is due to the explosive disintegration of the target, which produces the ejection of a mixture of vapor-phase molecules, small molecular clusters and droplets. To obtain smoother and uniform films, MAPLE deposition should be generally carried out at low laser fluency (a deposition laser power threshold is typically identified for each molecules/particles to be deposited), low repetition rate of laser pulses, low concentration of guest molecules in the target (typically 0.5-1 % wt.), large target-to-substrate distance (1-3 cm). Nevertheless, all these deposition parameters can be purposely tuned to achieve the optimal deposition conditions tailored for the molecules/particles to be deposited on a given substrate.

MAPLE approach has recently continuously evolving to cover a broad spectrum of organic, inorganic, and hybrid coatings for various biomedical applications as well as for energy, sensing, wearable electronics, and photonic devices [403-412]. MAPLE maturity readiness has already been achieved and commercial installations exist from PVD Products, Inc. (USA).

6 Conclusion

The importance of carbon-based nanomaterials has been increasing steadily in the past decades, in particular when it concerns the development of advanced materials for high demanding applications. Part of this interest arrives from the magnificent properties of these types of particles, that are able to introduce huge enhancements at low filler addition in composite materials. However, most of the potential utilizations of these particles have not moved yet from research to real application, in part due to obstacles mainly related with the reproducibility of properties and scalable production methodologies. Nowadays, there are several CNMs already commercially available in large quantities, in particular CNT and particles from the graphene family (graphene, GO, rGO). Nevertheless, the efficient dispersion of these types of particles in polymeric matrices is still a challenge, since it is common to obtain composite materials with CNMs agglomerates that act as defects and stress concentration points instead of providing multifunctionally and enhanced performance. Different strategies and methods are already available to facilitate the dispersion of CNM into different polymeric matrices, that are able to be used at industrial scale. For that reason, the following good practices and guidelines are recommended:

- Select the best type and amount of particle for each application

Depending on the requirements of the final material, different properties may be desired in detriment of others. For instance, GO and functionalized CNTs may present better affinity with polar polymeric matrices, facilitating its good dispersion and mechanical performance improvements. Nevertheless, properties, such as electrical conductivity, may be compromised and not suitable for sensing applications. Also, the amount of CNM needs to be optimized for the desired application, having in mind possible compromises between different properties. For example, increase the particle concentration may result in slightly decrease in terms of mechanical performance (compared to lower concentrations), but a great enhancement in the material sensitivity, or vice versa.

- Adapt dispersion method to the type of particle and matrix used

Since the CNM present different features, the dispersion methodology needs to be adapted to each particle and matrix used. This may include the combination of different strategies, such as functionalization with mechanical dispersion methods, or even two different mechanical methods, like sonication and calendaring.

- Optimize dispersion conditions for each type of particle since CNM from different providers present different properties and will behave differently in the matrix.

7 References

1. Asadian, E., M. Ghalkhani, and S. Shahrokhian, *Electrochemical sensing based on carbon nanoparticles: A review.* Sensors and Actuators B: Chemical, 2019. **293**: p. 183-209.

2. Mauter, M.S. and M. Elimelech, *Environmental Applications of Carbon-Based Nanomaterials.* Environmental Science & Technology, 2008. **42**(16): p. 5843-5859.

3. Pan, M., et al., *Carbon-Based Nanomaterials in Sensors for Food Safety.* 2019. **9**(9): p. 1330.

4. Kroto, H.W., et al., *C60: Buckminsterfullerene.* 1985. **318**(6042): p. 162-163.

5. Qiao, R., et al., *Translocation of C60 and its derivatives across a lipid bilayer.* 2007. **7**(3): p. 614-619.

6. Georgakilas, V., et al., *Broad family of carbon nanoallotropes: classification, chemistry, and applications of fullerenes, carbon dots, nanotubes, graphene, nanodiamonds, and combined superstructures.* 2015. **115**(11): p. 4744-4822.

7. Forró, L. and L.J.R.o.P.i.P. Mihály, *Electronic properties of doped fullerenes.* 2001. **64**(5): p. 649.

8. Karfunkel, H.R., T. Dressler, and A.J.J.o.c.-a.m.d. Hirsch, *Heterofullerenes: structure and property predictions, possible uses and synthesis proposals.* 1992. **6**(5): p. 521-535.

9. Muhr, H.-J., et al., *The boron heterofullerenes C59B and C69B: generation, extraction, mass spectrometric and XPS characterization.* 1996. **249**(5-6): p. 399-405.

10. Dunk, P.W., et al., *Formation of heterofullerenes by direct exposure of C60 to boron vapor.* 2013. **125**(1): p. 333-337.

11. Popov, A.A., S. Yang, and L.J.C.r. Dunsch, *Endohedral fullerenes.* 2013. **113**(8): p. 5989-6113.

12. Buseck, P.R., S.J. Tsipursky, and R. Hettich, *Fullerenes from the Geological Environment.* 1992. **257**(5067): p. 215-217.

13. Lieber, C.M. and C.-C. Chen, *Preparation of Fullerenes and Fullerene-Based Materials*, in *Solid State Physics*, H. Ehrenreich and F. Spaepen, Editors. 1994, Academic Press. p. 109-148.

14. Churilov, G.N., *Synthesis of Fullerenes and Other Nanomaterials in Arc Discharge.* Fullerenes, Nanotubes and Carbon Nanostructures, 2008. **16**(5-6): p. 395-403.

15. Shakirov, A.S., I.G. Galeev, and T. Ya Asadullin, *Features of formation of fullerene-containing soot during combustion gaseous and liquid hydrocarbons.* Journal of Physics: Conference Series, 2020. **1588**(1): p. 012013.

16. Ruoff, R., et al., *Solubility of fullerene (C60) in a variety of solvents.* 1993. **97**(13): p. 3379-3383.

17. Zhou, M., et al., *Electrochemical sensing platform based on the highly ordered mesoporous carbon− fullerene system.* 2008. **80**(12): p. 4642-4650.

18. Li, R., et al., *A novel glucose colorimetric sensor based on intrinsic peroxidase-like activity of C60-carboxyfullerenes.* 2013. **47**: p. 502-507.

19. Chuang, C.-W. and J.-S. Shih, *Preparation and application of immobilized C60-glucose oxidase enzyme in fullerene C60-coated piezoelectric quartz crystal glucose sensor.* Sensors and Actuators B: Chemical, 2001. **81**(1): p. 1-8.

20. Wei, L.-F. and J.-S. Shih, *Fullerene-cryptand coated piezoelectric crystal urea sensor based on urease.* Analytica Chimica Acta, 2001. **437**(1): p. 77-85.

21. Keshtkar, S., et al., *A novel highly sensitive and selective H2S gas sensor at low temperatures based on SnO2 quantum dots-C60 nanohybrid: Experimental and theory study.* Talanta, 2018. **188**: p. 531-539.

22. Ding, X., et al., *A QCM humidity sensor based on fullerene/graphene oxide nanocomposites with high quality factor.* Sensors and Actuators B: Chemical, 2018. **266**: p. 534-542.

23. Han, J., et al., *New Type of Redox Nanoprobe: C60-Based Nanomaterial and Its Application in Electrochemical Immunoassay for Doping Detection.* Analytical Chemistry, 2015. **87**(3): p. 1669-1675.

24. Goyal, R.N., et al., *Voltammetric Determination of Uric Acid at a Fullerene-C60-Modified Glassy Carbon Electrode.* 2005. **17**(24): p. 2217-2223.

25. Salazar, F.A., A. Fedorov, and M.N. Berberan-Santos, *A study of thermally activated delayed fluorescence in C60.* Chemical Physics Letters, 1997. **271**(4): p. 361-366.

26. Xu, X., et al., *Electrophoretic analysis and purification of fluorescent single-walled carbon nanotube fragments.* 2004. **126**(40): p. 12736-12737.

27. Baker, S.N. and G.A.J.A.C.I.E. Baker, *Luminescent carbon nanodots: emergent nanolights.* 2010. **49**(38): p. 6726-6744.

28. Wang, X., et al., *A mini review on carbon quantum dots: preparation, properties, and electrocatalytic application.* Frontiers in Chemistry, 2019: p. 671.

29. Cui, L., et al., *Carbon Dots: Synthesis, Properties and Applications.* Nanomaterials 2021. **11**(12): p. 3419.

30. Wu, Z.L., Z.X. Liu, and Y.H. Yuan, *Carbon dots: materials, synthesis, properties and approaches to long-wavelength and multicolor emission.* Journal of Materials Chemistry B, 2017. **5**(21): p. 3794-3809.

31. Demchenko, A.P., M.O.J.M. Dekaliuk, and a.i. fluorescence, *Novel fluorescent carbonic nanomaterials for sensing and imaging.* 2013. **1**(4): p. 042001.

32. Goryacheva, I.Y., A.V. Sapelkin, and G.B. Sukhorukov, *Carbon nanodots: Mechanisms of photoluminescence and principles of application.* TrAC Trends in Analytical Chemistry, 2017. **90**: p. 27-37.

33. Dong, Y., et al., *Polyamine-functionalized carbon quantum dots for chemical sensing.* 2012. **50**(8): p. 2810-2815.

34. Jana, J., et al., *One pot synthesis of intriguing fluorescent carbon dots for sensing and live cell imaging.* 2016. **150**: p. 253-264.

35. Algarra, M., et al., *Carbon dots obtained using hydrothermal treatment of formaldehyde. Cell imaging in vitro.* 2014. **6**(15): p. 9071-9077.

36. Zhu, S., et al., *Highly photoluminescent carbon dots for multicolor patterning, sensors, and bioimaging.* 2013. **125**(14): p. 4045-4049.

37. Parvin, N. and T.K.J.R.a. Mandal, *Synthesis of a highly fluorescence nitrogen-doped carbon quantum dots bioimaging probe and its in vivo clearance and printing applications.* 2016. **6**(22): p. 18134-18140.

38. Aguilera-Sigalat, J. and D. Bradshaw, *Synthesis and applications of metal-organic framework–quantum dot (QD@ MOF) composites.* Coordination Chemistry Reviews, 2016. **307**: p. 267-291.

39. Stepanidenko, E.A., et al., *Applications of carbon dots in optoelectronics.* Nanomaterials, 2021. **11**(2): p. 364.

40. Havrdova, M., et al., *Toxicity of carbon dots–Effect of surface functionalization on the cell viability, reactive oxygen species generation and cell cycle.* Carbon, 2016. **99**: p. 238-248.

41. Chan, M.-H., et al., *Natural Carbon Nanodots: Toxicity Assessment and Theranostic Biological Application.* Pharmaceutics, 2021. **13**(11): p. 1874.

42. Na, N., et al., *Application of fluorescent carbon nanodots in fluorescence imaging of human serum proteins.* 2013. **1**(6): p. 787-792.

43. Xu, B., et al., *Aptamer carbon nanodot sandwich used for fluorescent detection of protein.* 2012. **137**(23): p. 5483-5486.

44. Mandal, T.K. and N.J.J.o.b.n. Parvin, *Rapid detection of bacteria by carbon quantum dots.* 2011. **7**(6): p. 846-848.

45. Kong, B., et al., *Carbon dot-based inorganic–organic nanosystem for two-photon imaging and biosensing of pH variation in living cells and tissues.* 2012. **24**(43): p. 5844-5848.

46. Gonçalves, H., et al., *Hg (II) sensing based on functionalized carbon dots obtained by direct laser ablation.* 2010. **145**(2): p. 702-707.

47. Iijima, S.J.n., *Helical microtubules of graphitic carbon.* 1991. **354**(6348): p. 56-58.

48. Iijima, S. and T.J.n. Ichihashi, *Single-shell carbon nanotubes of 1-nm diameter.* 1993. **363**(6430): p. 603-605.

49. Hirahara, K., et al., *Stretching of carbon-carbon bonds in a 0.7 nm diameter carbon nanotube studied by electron diffraction.* 2004. **70**(20): p. 205422.

50. Yu, M.-F., et al., *Strength and breaking mechanism of multiwalled carbon nanotubes under tensile load.* 2000. **287**(5453): p. 637-640.

51. Poncharal, P., et al., *Room temperature ballistic conduction in carbon nanotubes*. 2002, ACS Publications. p. 12104-12118.

52. Saifuddin, N., A. Raziah, and A.J.J.o.C. Junizah, *Carbon nanotubes: a review on structure and their interaction with proteins.* 2013. **2013**.

53. Zaporotskova, I.V., et al., *Carbon nanotubes: Sensor properties. A review.* 2016. **2**(4): p. 95-105.

54. Dai, H., *Nanotube growth and characterization*, in *Carbon Nanotubes*. 2001, Springer. p. 29-53.

55. Ding, L., et al., *Selective growth of well-aligned semiconducting single-walled carbon nanotubes.* 2009. **9**(2): p. 800-805.

56. Chegel, R.J.P.B.C.M., *Tuning electronic properties of carbon nanotubes by Boron and Nitrogen doping.* 2016. **499**: p. 1-16.

57. Janas, D., et al., *Improving the electrical properties of carbon nanotubes with interhalogen compounds.* 2017. **9**(9): p. 3212-3221.

58. Dai, H.J.A.o.c.r., *Carbon nanotubes: synthesis, integration, and properties.* 2002. **35**(12): p. 1035-1044.

59. Chen, A. and S.J.C.S.R. Chatterjee, *Nanomaterials based electrochemical sensors for biomedical applications.* 2013. **42**(12): p. 5425-5438.

60. Jovanović, S.P., et al., *A novel method for the functionalization of γ-irradiated single wall carbon nanotubes with DNA.* 2009. **20**(44): p. 445602.

61. Schroeder, V., et al., *Carbon nanotube chemical sensors.* 2018. **119**(1): p. 599-663.

62. De Jong, K.P. and J.W. Geus, *Carbon Nanofibers: Catalytic Synthesis and Applications.* Catalysis Reviews, 2000. **42**(4): p. 481-510.

63. Shoukat, R. and M.I.J.E.E. Khan, *Synthesis of vertically aligned carbon nanofibers using inductively coupled plasma-enhanced chemical vapor deposition.* 2018. **100**(2): p. 997-1002.

64. Chiang, Y.-C., W.-T. Chin, and C.-C.J.P. Huang, *The Application of Hollow Carbon Nanofibers Prepared by Electrospinning to Carbon Dioxide Capture.* 2021. **13**(19): p. 3275.

65. Zou, G., et al., *Carbon nanofibers: Synthesis, characterization, and electrochemical properties.* Carbon, 2006. **44**(5): p. 828-832.

66. Rand, E., et al., *A carbon nanofiber based biosensor for simultaneous detection of dopamine and serotonin in the presence of ascorbicacid.* 2013. **42**: p. 434-438.

67. Yue, Y., et al., *A mesoporous carbon nanofiber-modified pyrolytic graphite electrode used for the simultaneous determination of dopamine, uric acid, and ascorbic acid.* 2012. **50**(1): p. 107-114.

68. Yadav, D., F. Amini, and A. Ehrmann, *Recent advances in carbon nanofibers and their applications – A review.* European Polymer Journal, 2020. **138**: p. 109963.

69. Wang, Z., et al., *Carbon nanofiber-based functional nanomaterials for sensor applications.* 2019. **9**(7): p. 1045.

70. Meng, Y., *Polymer/graphite nanocomposites*, in *Polymer nanocomposites*, Y.-W. Mai and Z.-Z. Yu, Editors. 2006, CRC Press: Cambridge UK.

71. Warner, J.H., et al., *Graphene: Fundamentals and emergent applications*. 2012: Newnes.

72. Burchell, T.D. and T.R. Pavlov, *Graphite: Properties and Characteristics* in *Comprehensive nuclear materials*, R.J. Konings and R. Stoller, Editors. 2020, Elsevier.

73. Batten, S.R., et al., *Terminology of metal–organic frameworks and coordination polymers (IUPAC Recommendations 2013).* Pure Applied Chemistry, 2013. **85**(8): p. 1715-1724.

74. Ergun, S., *Structure of graphite.* Nature physical science, 1973. **241**(107): p. 65-67.

75. Inagaki, M., *Applications of graphite intercalation compounds.* Journal of Materials Research, 1989. **4**(6): p. 1560-1568.

76. Xu, J., et al., *Recent progress in graphite intercalation compounds for rechargeable metal (Li, Na, K, Al)-ion batteries.* Advanced Science, 2017. **4**(10): p. 1700146.

77. Novoselov, K., et al., *Room-temperature electric field effect and carrier-type inversion in graphene films.* preprint cond-mat/0410631, 2004.

78. Hansora, D., N. Shimpi, and S. Mishra, *Graphite to graphene via graphene oxide: an overview on synthesis, properties, and applications.* Jom, 2015. **67**(12): p. 2855-2868.

79. Bhuyan, M., et al., *Synthesis of graphene.* International Nano Letters, 2016. **6**(2): p. 65-83.

80. Sun, Y., et al., *Mechanical properties of graphene.* Applied Physics Reviews, 2021. **8**(2): p. 021310.

81. Skoda, M., et al., *Graphene: one material, many possibilities—application difficulties in biological systems.* Journal of Nanomaterials, 2014. **2014**.

82. Backes, C., et al., *Production and processing of graphene and related materials.* 2D Materials, 2020. **7**(2): p. 022001.

83. Edwards, R.S. and K.S. Coleman, *Graphene synthesis: relationship to applications.* Nanoscale, 2013. **5**(1): p. 38-51.

84. Tarcan, R., et al., *Reduced graphene oxide today.* Journal of Materials Chemistry C, 2020. **8**(4): p. 1198-1224.

85. Yi, M. and Z. Shen, *A review on mechanical exfoliation for the scalable production of graphene.* Journal of Materials Chemistry A, 2015. **3**(22): p. 11700-11715.

86. Munoz, R. and C. Gómez-Aleixandre, *Review of CVD synthesis of graphene.* Chemical Vapor Deposition, 2013. **19**(10-11-12): p. 297-322.

87. Avouris, P. and C. Dimitrakopoulos, *Graphene: synthesis and applications.* Materials today, 2012. **15**(3): p. 86-97.

88. Olabi, A., et al., *Application of graphene in energy storage device–A review.* Renewable Sustainable Energy Reviews, 2021. **135**: p. 110026.

89. Priyadarsini, S., et al., *Graphene and graphene oxide as nanomaterials for medicine and biology application.* Journal of Nanostructure in Chemistry, 2018. **8**(2): p. 123-137.

90. Tung, T.T., et al., *Recent advances in sensing applications of graphene assemblies and their composites.* Advanced Functional Materials, 2017. **27**(46): p. 1702891.

91. Phiri, J., P. Gane, and T.C. Maloney, *General overview of graphene: Production, properties and application in polymer composites.* Materials Science and Engineering: B, 2017. **215**: p. 9-28.

92. Bablich, A., S. Kataria, and M.C. Lemme, *Graphene and two-dimensional materials for optoelectronic applications.* Electronics, 2016. **5**(1): p. 13.

93. Bianco, A., et al., *All in the graphene family – A recommended nomenclature for two-dimensional carbon materials.* Carbon, 2013. **65**: p. 1-6.

94. Li, Y., et al., *In situ exfoliation of graphene in epoxy resins: a facile strategy to efficient and large scale graphene nanocomposites.* 2016. **8**(36): p. 24112-24122.

95. Gong, L., et al., *Optimizing the Reinforcement of Polymer-Based Nanocomposites by Graphene.* ACS Nano, 2012. **6**(3): p. 2086-2095.

96. Yu, W., et al., *Progress in the functional modification of graphene/graphene oxide: A review.* 2020. **10**(26): p. 15328-15345.

97. Perrozzi, F., S. Prezioso, and L. Ottaviano, *Graphene oxide: from fundamentals to applications.* Journal of Physics: Condensed Matter, 2014. **27**(1): p. 013002.

98. Dreyer, D.R., et al., *The chemistry of graphene oxide.* Chemical society reviews, 2010. **39**(1): p. 228-240.

99. Lerf, A., et al., *Structure of graphite oxide revisited.* The Journal of Physical Chemistry B, 1998. **102**(23): p. 4477-4482.

100. Erickson, K., et al., *Determination of the local chemical structure of graphene oxide and reduced graphene oxide.* Advanced materials, 2010. **22**(40): p. 4467-4472.

101. Neklyudov, V.V., et al., *New insights into the solubility of graphene oxide in water and alcohols.* Physical Chemistry Chemical Physics, 2017. **19**(26): p. 17000-17008.

102. Konios, D., et al., *Dispersion behaviour of graphene oxide and reduced graphene oxide.* Journal of colloid interface science, 2014. **430**: p. 108-112.

103. Dideikin, A.T. and A.Y. Vul', *Graphene oxide and derivatives: the place in graphene family.* Frontiers in Physics, 2019. **6**: p. 149.

104. Smith, A.T., et al., *Synthesis, properties, and applications of graphene oxide/reduced graphene oxide and their nanocomposites.* Nano Materials Science, 2019. **1**(1): p. 31-47.

105. Hummers Jr, W.S. and R.E.J.J.o.t.a.c.s. Offeman, *Preparation of graphitic oxide.* 1958. **80**(6): p. 1339-1339.

106. Marcano, D.C., et al., *Improved synthesis of graphene oxide.* ACS nano, 2010. **4**(8): p. 4806-4814.

107. Kovtyukhova, N.I., et al., *Layer-by-layer assembly of ultrathin composite films from micron-sized graphite oxide sheets and polycations.* Chemistry of materials, 1999. **11**(3): p. 771-778.

108. Sun, L. and B. Fugetsu, *Mass production of graphene oxide from expanded graphite.* Materials Letters, 2013. **109**: p. 207-210.

109. Yu, C., C.-F. Wang, and S.J.S.r. Chen, *Facile access to graphene oxide from ferro-induced oxidation.* 2016. **6**(1): p. 1-7.

110. Peng, L., et al., *An iron-based green approach to 1-h production of single-layer graphene oxide.* Nature communications, 2015. **6**(1): p. 1-9.

111. Stankovich, S., et al., *Synthesis of graphene-based nanosheets via chemical reduction of exfoliated graphite oxide.* Carbon, 2007. **45**(7): p. 1558-1565.

112. Chua, C.K. and M. Pumera, *Chemical reduction of graphene oxide: a synthetic chemistry viewpoint.* Chemical Society Reviews, 2014. **43**(1): p. 291-312.

113. Sengupta, I., et al., *Thermal reduction of graphene oxide: How temperature influences purity.* Journal of Materials Research, 2018. **33**(23): p. 4113-4122.

114. Chen, W., L. Yan, and P.R. Bangal, *Preparation of graphene by the rapid and mild thermal reduction of graphene oxide induced by microwaves.* Carbon, 2010. **48**(4): p. 1146-1152.

115. Williams, G., B. Seger, and P.V. Kamat, *TiO2-graphene nanocomposites. UV-assisted photocatalytic reduction of graphene oxide.* ACS nano, 2008. **2**(7): p. 1487-1491.

116. Shao, Y., et al., *Facile and controllable electrochemical reduction of graphene oxide and its applications.* Journal of Materials Chemistry 2010. **20**(4): p. 743-748.

117. Kan, E.-j., et al., *Half-Metallicity in Edge-Modified Zigzag Graphene Nanoribbons.* Journal of the American Chemical Society, 2008. **130**(13): p. 4224-4225.

118. Zheng, H., et al., *Analytical study of electronic structure in armchair graphene nanoribbons.* 2007. **75**(16): p. 165414.

119. Ma, L., J. Wang, and F. Ding, *Recent Progress and Challenges in Graphene Nanoribbon Synthesis.* 2013. **14**(1): p. 47-54.

120. Corso, M., et al., *Chapter Bottom-Up Fabrication of Atomically Precise Graphene Nanoribbons*, in *On-Surface Synthesis II*. 2018, Springer Nature.

121. Zhang, R., et al., *Graphene Nanoribbon-Supported PtPd Concave Nanocubes for Electrochemical Detection of TNT with High Sensitivity and Selectivity.* Analytical Chemistry, 2015. **87**(24): p. 12262-12269.

122. Huang, B., et al., *Adsorption of Gas Molecules on Graphene Nanoribbons and Its Implication for Nanoscale Molecule Sensor.* The Journal of Physical Chemistry C, 2008. **112**(35): p. 13442-13446.

123. Martín, A., et al., *Controlled chemistry of tailored graphene nanoribbons for electrochemistry: a rational approach to optimizing molecule detection.* 2014. **4**(1): p. 132-139.

124. Jaiswal, N.K., G. Kovačević, and B.J.A.S.S. Pivac, *Reconstructed graphene nanoribbon as a sensor for nitrogen based molecules.* 2015. **357**: p. 55-59.

125. Salih, E., A.I.J.P.E.L.-d.S. Ayesh, and Nanostructures, *Pt-doped armchair graphene nanoribbon as a promising gas sensor for CO and CO2: DFT study.* 2021. **125**: p. 114418.

126. Wang, T., et al., *Top-down synthesis of graphene nanoribbons using different sources of carbon nanotubes.* 2020. **158**: p. 615-623.

127. Dobrik, G., et al., *Crystallographically oriented high resolution lithography of graphene nanoribbons by STM lithography.* 2010. **247**(4): p. 896-902.

128. Chen, Z., et al., *Synthesis of graphene nanoribbons by ambient-pressure chemical vapor deposition and device integration.* 2016. **138**(47): p. 15488-15496.

129. Alfè, M., et al., *Wet chemical method for making graphene-like films from carbon black.* ACS applied materials interfaces, 2012. **4**(9): p. 4491-4498.

130. Alfè, M., V. Gargiulo, and R. Di Capua, *Tuning the surface morphology of self-assembled graphene-like thin films through pH variation.* Applied Surface Science, 2015. **353**: p. 628-635.

131. Gargiulo, V., et al., *Graphene-like layers as promising chemiresistive sensing material for detection of alcohols at low concentration.* Journal of Applied Physics, 2018. **123**(2): p. 024503.

132. Di Capua, R., et al., *Eumelanin graphene-like integration: The impact on physical properties and electrical conductivity.* Frontiers in chemistry, 2019. **7**: p. 121.

133. Alfè, M., et al., *Synthesis and characterization of conductive copper-based metal-organic framework/graphene-like composites.* Materials Chemistry Physics, 2014. **147**(3): p. 744-750.

134. Alfe, M., et al., *Solid sorbents for CO2 and CH4 adsorption: The effect of metal organic framework hybridization with graphene-like layers on the gas sorption capacities at high pressure.* Renewable Sustainable Energy Reviews, 2021. **141**: p. 110816.

135. Gargiulo, V., et al., *Supplementing π-systems: Eumelanin and graphene-like integration towards highly conductive materials for the mammalian cell culture bio-interface.* Journal of Materials Chemistry B, 2015. **3**(25): p. 5070-5079.

136. Papari, G.P., et al., *THz spectroscopy on graphene-like materials for bio-compatible devices.* Journal of Applied Physics, 2017. **121**(14): p. 145107.

137. Lettieri, S., et al., *Evidencing opposite charge-transfer processes at TiO2/graphene-related materials interface through a combined EPR, photoluminescence and photocatalysis assessment.* Catalysis Today, 2018. **315**: p. 19-30.

138. Olivi, M., et al., *Antimicrobial properties of graphene-like nanoparticles: coating effect on Staphylococcus aureus.* Journal of Nanoparticle Research, 2016. **18**(12): p. 1-10.

139. d'Amora, M., et al., *Graphene-like layers from carbon black: In vivo toxicity assessment.* Nanomaterials, 2020. **10**(8): p. 1472.

140. Villani, F., et al. *Graphene-like based-chemiresistors inkjet-printed onto paper substrate*. in *Convegno Nazionale Sensori*. 2018. Springer.

141. Ali, Z. *Global Industry Analysts Predicts the World Biochar Market to Reach $2 Billion by 2026*. 2022 30 April 2022]; Available from: https://www.prnewswire.com/news-releases/global-industry-analysts-predicts-the-world-biochar-market-to-reach-2-billion-by-2026-301461859.html.

142. Chen, N. and S. Pilla, *A comprehensive review on transforming lignocellulosic materials into biocarbon and its utilization for composites applications.* Composites Part C: Open Access, 2022. **7**: p. 100225.

143. Behazin, E., M. Misra, and A.K. Mohanty, *Sustainable biocarbon from pyrolyzed perennial grasses and their effects on impact modified polypropylene biocomposites.* Composites Part B: Engineering, 2017. **118**: p. 116-124.

144. Kong, X., et al., *Synthesis of graphene-like carbon from biomass pyrolysis and its applications.* Chemical Engineering Journal, 2020. **399**: p. 125808.

145. Çavdar, A.D., *New generation Carbon Materials "Biochar"*, in *Academic Studies in Agriculture, Forestry and Aquaculture Sciences - II*, A. Bolat, Editor. 2020, Gece Publishing: Ankara. p. 211-220.

146. Basta, A., et al., *2-Steps KOH activation of rice straw: an efficient method for preparing high-performance activated carbons.* 2009. **100**(17): p. 3941-3947.

147. Wang, J. and S.J.J.o.M.C. Kaskel, *KOH activation of carbon-based materials for energy storage.* 2012. **22**(45): p. 23710-23725.

148. Otowa, T., Y. Nojima, and T.J.C. Miyazaki, *Development of KOH activated high surface area carbon and its application to drinking water purification.* 1997. **35**(9): p. 1315-1319.

149. Abdelwahab, M.A., et al., *Injection Molded Novel Biocomposites from Polypropylene and Sustainable Biocarbon.* Molecules, 2019. **24**(22).

150. Wang, T., et al., *Sustainable carbonaceous biofiller from miscanthus: Size reduction, characterization, and potential bio-composites applications.* 2018. **13**(2): p. 3720-3739.

151. Snowdon, M.R., et al., *Comparative study of the extrinsic properties of poly(lactic acid)-based biocomposites filled with talc versus sustainable biocarbon.* RSC Advances, 2019. **9**(12): p. 6752-6761.

152. Rizal, S., et al., *Propionic Anhydride Modification of Cellulosic Kenaf Fibre Enhancement with Bionanocarbon in Nanobiocomposites.* Molecules, 2021. **26**(14).

153. Rizal, S., et al., *Functional Properties of Kenaf Bast Fibre Anhydride Modification Enhancement with Bionanocarbon in Polymer Nanobiocomposites.* Polymers (Basel), 2021. **13**(23).

154. Peterson, S.C., et al., *Increasing biochar surface area: Optimization of ball milling parameters.* Powder Technology, 2012. **228**: p. 115-120.

155. Safian, M.T.-u., U.S. Haron, and M.M. Ibrahim, *A review on bio-based graphene derived from biomass wastes.* BioResources, 2020. **15**(4): p. 9756.

156. Raghavan, N., S. Thangavel, and G. Venugopal, *A short review on preparation of graphene from waste and bioprecursors.* Applied Materials Today, 2017. **7**: p. 246-254.

157. You, X., et al., *Preparation of an Electric Double Layer Capacitor (EDLC) Using Miscanthus-Derived Biocarbon.* ACS Sustainable Chemistry & Engineering, 2017. **6**(1): p. 318-324.

158. Rizal, S., et al., *Bionanocarbon Functional Material Characterisation and Enhancement Properties in Nonwoven Kenaf Fibre Nanocomposites.* Polymers (Basel), 2021. **13**(14).

159. Mousa, M. and Y. Dong, *Strong Poly(Vinyl Alcohol) (PVA)/Bamboo Charcoal (BC) Nanocomposite Films with Particle Size Effect.* ACS Sustainable Chemistry & Engineering, 2017. **6**(1): p. 467-479.

160. Purkait, T., et al., *Large area few-layer graphene with scalable preparation from waste biomass for high-performance supercapacitor.* Sci Rep, 2017. **7**(1): p. 15239.

161. Sun, L., et al., *From coconut shell to porous graphene-like nanosheets for high-power supercapacitors.* Journal of Materials Chemistry A, 2013. **1**(21).

162. Ben-Yoav, H., M. A. Schroeder, and M. Noked, *Chitosan bio-functionalization of carbon nanotube arrayed electrode.* Advanced Materials Letters, 2017. **8**(12): p. 1166-1170.

163. Suriani, A.B., et al., *Scaled-up prototype of carbon nanotube production system utilizing waste cooking palm oil precursor and its nanocomposite application as supercapacitor electrodes.* Journal of Materials Science: Materials in Electronics, 2016. **27**(11): p. 11599-11605.

164. Yusof, J.M., et al., *Effect of zinc oxide nucleation on flexible bio based carbon nanotube cotton via chemical bath deposition method.* Microelectronic Engineering, 2020. **234**.

165. Li, S., et al., *Flexible cellulose based polypyrrole–multiwalled carbon nanotube films for bio-compatible zinc batteries activated by simulated body fluids.* 2013. **1**(45): p. 14300-14305.

166. Suppiah, K., et al., *The Mechanical Properties of Carboxymethyl Cellulose (CMC) Filled Halloysite Nanotube (HNT) Bio-Nanocomposite Films: Effect of Sodium Dodecyl Sulfate (SDS).* Solid State Phenomena, 2018. **280**: p. 335-339.

167. Gonugunta, P., *Synthesis and Characterization of biobased carbon nanoparticles from Lignin*. 2012, University of Guelph.

168. Ikram, R., et al., *Advances in synthesis of graphene derivatives using industrial wastes precursors; prospects and challenges.* Journal of Materials Research 2020. **9**(6): p. 15924-15951.

169. Vieira, O., et al., *A systematic literature review on the conversion of plastic wastes into valuable 2D graphene-based materials.* Chemical Engineering Journal, 2022. **428**: p. 131399.

170. Poorna, A., R. Saravanathamizhan, and N. Balasubramanian, *Graphene and graphene-like structure from biomass for Electrochemical Energy Storage application-A Review.* Electrochemical Science Advances, 2021. **1**(3): p. e2000028.

171. Sierra, U., et al., *New alternatives to graphite for producing graphene materials.* Carbon, 2015. **93**: p. 812-818.

172. Sierra, U., et al., *Cokes of different origin as precursors of graphene oxide.* Fuel, 2016. **166**: p. 400-403.

173. Sierra, U., et al., *Coke-derived few layer graphene-like materials by mild planetary milling exfoliation.* Fuel, 2020. **262**: p. 116455.

174. Saha, S., et al., *Sustainable production of graphene from petroleum coke using electrochemical exfoliation.* 2D Materials

Applications

2021. **5**(1): p. 1-8.

175. Ali-Akbari, H.R., S. Ceballes, and A. Abdelkefi, *Nonlinear performance analysis of forced carbon nanotube-based bio-mass sensors.* International Journal of Mechanics and Materials in Design, 2018. **15**(2): p. 291-315.

176. Wei, J., et al., *Green Carbon Nanofiber Networks for Advanced Energy Storage.* ACS Applied Energy Materials, 2020. **3**(4): p. 3530-3540.

177. Gu, H., et al., *An overview of multifunctional epoxy nanocomposites.* 2016. **4**(25): p. 5890-5906.

178. Araujo, A., et al. *Challenges and opportunities on nano-enabled multifunctional composites for aerostructures*. in *MATEC Web of Conferences*. 2019. EDP Sciences.

179. Garg, M., S. Sharma, and R. Mehta, *Pristine and amino functionalized carbon nanotubes reinforced glass fiber epoxy composites.* Composites Part A: Applied Science and Manufacturing, 2015. **76**: p. 92-101.

180. Jojibabu, P., Y.X. Zhang, and B.G. Prusty, *A review of research advances in epoxy-based nanocomposites as adhesive materials.* International Journal of Adhesion and Adhesives, 2020. **96**.

181. Lavagna, L., et al., *Functionalization as a way to enhance dispersion of carbon nanotubes in matrices: a review.* Materials Today Chemistry, 2021. **20**.

182. Ma, P.-C., et al., *Dispersion and functionalization of carbon nanotubes for polymer-based nanocomposites: A review.* Composites Part A: Applied Science and Manufacturing, 2010. **41**(10): p. 1345-1367.

183. Gardea, F. and D.C. Lagoudas, *Characterization of electrical and thermal properties of carbon nanotube/epoxy composites.* Composites Part B: Engineering, 2014. **56**: p. 611-620.

184. Jagtap, S.B. and D. Ratna, *Preparation and characterization of rubbery epoxy/multiwall carbon nanotubes composites using amino acid salt assisted dispersion technique.* Express Polymer Letters, 2013. **7**(4): p. 329-339.

185. Uzunpinar, C., M.A. Mosiewicki, and M.L. Auad, *Effect of SWCNT dispersion on epoxy nanocomposite properties.* Polymer Composites, 2012. **33**(4): p. 582-588.

186. Pizzutto, C.E., et al., *Study of epoxy/CNT nanocomposites prepared via dispersion in the hardener.* Materials Research, 2011. **14**(2): p. 256-263.

187. Bansal, S.A., et al., *Small percentage reinforcement of carbon nanotubes (CNTs) in epoxy(bisphenol-A) for enhanced mechanical performance.* Materials Today: Proceedings, 2021.

188. Pizzutto, C.E., et al., *Mechanical and Dilatometric Properties of Carboxylated SWCNT/Epoxy Composites: Effects of the Dispersion in the Resin and in the Hardener.* Journal of Reinforced Plastics and Composites, 2009. **29**(4): p. 524-530.

189. Zhou, Y., M.I. Jeelani, and S. Jeelani, *Development of photo micro-graph method to characterize dispersion of CNT in epoxy.* Materials Science and Engineering: A, 2009. **506**(1-2): p. 39-44.

190. Rana, S., R. Alagirusamy, and M. Joshi, *Effect of carbon nanofiber dispersion on the tensile properties of epoxy nanocomposites.* Journal of Composite Materials, 2011. **45**(21): p. 2247-2256.

191. Sun, L.-H., et al., *Preparation, Characterization, and Modeling of Carbon Nanofiber/Epoxy Nanocomposites.* Journal of Nanomaterials, 2011. **2011**: p. 307589.

192. Prolongo, S.G., et al., *Effects of dispersion techniques of carbon nanofibers on the thermo-physical properties of epoxy nanocomposites.* Composites Science and Technology, 2008. **68**(13): p. 2722-2730.

193. Monti, M., et al., *Morphology and electrical properties of graphene–epoxy nanocomposites obtained by different solvent assisted processing methods.* Composites Part A: Applied Science and Manufacturing, 2013. **46**: p. 166-172.

194. Liu, K., et al., *Edge-functionalized graphene as reinforcement of epoxy-based conductive composite for electrical interconnects.* Composites Science and Technology, 2013. **88**: p. 84-91.

195. Wajid, A.S., et al., *High-Performance Pristine Graphene/Epoxy Composites With Enhanced Mechanical and Electrical Properties.* Macromolecular Materials and Engineering, 2013. **298**(3): p. 339-347.

196. Wei, J., et al., *Graphene Nanoplatelets in Epoxy System: Dispersion, Reaggregation, and Mechanical Properties of Nanocomposites.* Journal of Nanomaterials, 2015. **2015**: p. 1-12.

197. Pokharel, P., Q.-T. Truong, and D.S. Lee, *Multi-step microwave reduction of graphite oxide and its use in the formation of electrically conductive graphene/epoxy composites.* Composites Part B: Engineering, 2014. **64**: p. 187-193.

198. Li, A., C. Zhang, and Y.-F. Zhang, *Graphene nanosheets-filled epoxy composites prepared by a fast dispersion method.* Journal of Applied Polymer Science, 2017. **134**(36).

199. Aradhana, R., S. Mohanty, and S.K. Nayak, *Comparison of mechanical, electrical and thermal properties in graphene oxide and reduced graphene oxide filled epoxy nanocomposite adhesives.* Polymer, 2018. **141**: p. 109-123.

200. Rafiei Hashjin, R.n., Z. Ranjbar, and H. Yari, *Modeling of electrical conductive graphene filled epoxy coatings.* Progress in Organic Coatings, 2018. **125**: p. 411-419.

201. Esmaeili, A., et al., *Strain and crack growth sensing capability of SWCNT reinforced epoxy in tensile and mode I fracture tests.* Composites Science and Technology, 2020. **186**.

202. Bouhamed, A., et al., *Processing and characterization of MWCNTs/epoxy nanocomposites thin films for strain sensing applications.* Sensors and Actuators A: Physical, 2017. **257**: p. 65-72.

203. Kumar, A., et al., *Thermo-mechanical and anti-corrosive properties of MWCNT/epoxy nanocomposite fabricated by innovative dispersion technique.* Composites Part B: Engineering, 2017. **113**: p. 291-299.

204. Tang, L.-C., et al., *The effect of graphene dispersion on the mechanical properties of graphene/epoxy composites.* Carbon, 2013. **60**: p. 16-27.

205. Li, Y., et al., *Mechanical, electrical and thermal properties of in-situ exfoliated graphene/epoxy nanocomposites.* Composites Part A: Applied Science and Manufacturing, 2017. **95**: p. 229-236.

206. Frømyr, T.R., F.K. Hansen, and T. Olsen, *The Optimum Dispersion of Carbon Nanotubes for Epoxy Nanocomposites: Evolution of the Particle Size Distribution by Ultrasonic Treatment.* Journal of Nanotechnology, 2012. **2012**: p. 1-14.

207. Gkikas, G., N.M. Barkoula, and A.S. Paipetis, *Effect of dispersion conditions on the thermo-mechanical and toughness properties of multi walled carbon nanotubes-reinforced epoxy.* Composites Part B: Engineering, 2012. **43**(6): p. 2697-2705.

208. An, J.-E. and Y.G. Jeong, *Structure and electric heating performance of graphene/epoxy composite films.* European Polymer Journal, 2013. **49**(6): p. 1322-1330.

209. Rennhofer, H. and B. Zanghellini, *Dispersion State and Damage of Carbon Nanotubes and Carbon Nanofibers by Ultrasonic Dispersion: A Review.* Nanomaterials (Basel), 2021. **11**(6).

210. Chang, L., et al., *Evaluation and visualization of the percolating networks in multi-wall carbon nanotube/epoxy composites.* Journal of Materials Science, 2009. **44**(15): p. 4003-4012.

211. Srivastava, V.K., *Modeling and mechanical performance of carbon nanotube/epoxy resin composites.* Materials & Design, 2012. **39**: p. 432-436.

212. Yang, H., et al., *Multi-scale study of CNT and CNT-COOH reinforced epoxy composites: dispersion state, interfacial interaction vs mechanical properties.* Composite Interfaces, 2020. **28**(4): p. 381-393.

213. Thostenson, E.T. and T.-W. Chou, *Processing-structure-multi-functional property relationship in carbon nanotube/epoxy composites.* Carbon, 2006. **44**(14): p. 3022-3029.

214. Gojny, F., et al., *Influence of different carbon nanotubes on the mechanical properties of epoxy matrix composites – A comparative study.* Composites Science and Technology, 2005. **65**(15-16): p. 2300-2313.

215. Ladani, R.B., et al., *Improving the toughness and electrical conductivity of epoxy nanocomposites by using aligned carbon nanofibres.* Composites Science and Technology, 2015. **117**: p. 146-158.

216. Chandrasekaran, S., C. Seidel, and K. Schulte, *Preparation and characterization of graphite nano-platelet (GNP)/epoxy nano-composite: Mechanical, electrical and thermal properties.* European Polymer Journal, 2013. **49**(12): p. 3878-3888.

217. Chandrasekaran, S., et al., *Fracture toughness and failure mechanism of graphene based epoxy composites.* Composites Science and Technology, 2014. **97**: p. 90-99.

218. Ravindran, A.R., et al., *Effects of Graphene Nanoplatelet Size and Surface Area on the AC Electrical Conductivity and Dielectric Constant of Epoxy Nanocomposites.* Polymers (Basel), 2018. **10**(5).

219. Vazquez-Moreno, J.M., et al., *Customizing thermally-reduced graphene oxides for electrically conductive or mechanical reinforced epoxy nanocomposites.* European Polymer Journal, 2017. **93**: p. 1-7.

220. Pras, M., et al., *Key Role of the Dispersion of Carbon Nanotubes (CNTs) within Epoxy Networks on their Ability to Release.* Polymers (Basel), 2020. **12**(11).

221. Campo, M., A. Jiménez-Suárez, and A. Ureña, *Effect of type, percentage and dispersion method of multi-walled carbon nanotubes on tribological properties of epoxy composites.* Wear, 2015. **324-325**: p. 100-108.

222. Imran, K.A. and K.N. Shivakumar, *Enhancement of electrical conductivity of epoxy using graphene and determination of their thermo-mechanical properties.* Journal of Reinforced Plastics and Composites, 2017. **37**(2): p. 118-133.

223. Prolongo, S.G., et al., *Advantages and disadvantages of the addition of graphene nanoplatelets to epoxy resins.* European Polymer Journal, 2014. **61**: p. 206-214.

224. Wu, S., et al., *Aligning multilayer graphene flakes with an external electric field to improve multifunctional properties of epoxy nanocomposites.* Carbon, 2015. **94**: p. 607-618.

225. Moriche, R., et al., *Morphological changes on graphene nanoplatelets induced during dispersion into an epoxy resin by different methods.* Composites Part B: Engineering, 2015. **72**: p. 199-205.

226. Wang, F., et al., *Mechanical properties and thermal conductivity of graphene nanoplatelet/epoxy composites.* Journal of Materials Science, 2014. **50**(3): p. 1082-1093.

227. Ladani, R.B., et al., *Multifunctional properties of epoxy nanocomposites reinforced by aligned nanoscale carbon.* Materials & Design, 2016. **94**: p. 554-564.

228. Huang, X., et al., *A multifunctional carbon nanotube reinforced nanocomposite modified via soy protein isolate: A study on dispersion, electrical and mechanical properties.* Carbon, 2020. **161**: p. 350-358.

229. Jin, F.-L., C.-J. Ma, and S.-J. Park, *Thermal and mechanical interfacial properties of epoxy composites based on functionalized carbon nanotubes.* Materials Science and Engineering: A, 2011. **528**(29-30): p. 8517-8522.

230. Guo, P., et al., *Fabrication and mechanical properties of well-dispersed multiwalled carbon nanotubes/epoxy composites.* Composites Science and Technology, 2007. **67**(15-16): p. 3331-3337.

231. Brodie, B.C.J.P.t.o.t.R.S.o.L., *XIII. On the atomic weight of graphite.* 1859(149): p. 249-259.

232. Wei, J., T. Vo, and F. Inam, *Epoxy/graphene nanocomposites – processing and properties: a review.* RSC Advances, 2015. **5**(90): p. 73510-73524.

233. Tiwari, M., et al., *Quantification of carbon nanotube dispersion and its correlation with mechanical and thermal properties of epoxy nanocomposites.* Journal of Applied Polymer Science, 2019. **137**(29).

234. Ma, P.-C., et al., *Dispersion, interfacial interaction and re-agglomeration of functionalized carbon nanotubes in epoxy composites.* Carbon, 2010. **48**(6): p. 1824-1834.

235. Yang, K. and M. Gu, *The effects of triethylenetetramine grafting of multi-walled carbon nanotubes on its dispersion, filler-matrix interfacial interaction and the thermal properties of epoxy nanocomposites.* Polymer Engineering & Science, 2009. **49**(11): p. 2158-2167.

236. Wang, J., et al., *Effect of amino-functionalization of multi-walled carbon nanotubes on the dispersion with epoxy resin matrix.* Journal of Applied Polymer Science, 2006. **100**(1): p. 97-104.

237. Mostovoy, A., et al., *Epoxy Nanocomposites Reinforced with Functionalized Carbon Nanotubes.* Polymers (Basel), 2020. **12**(8).

238. Armstrong, G., et al., *Functionalised multi-walled carbon nanotubes for epoxy nanocomposites with improved performance.* Polymer International, 2009. **58**(9): p. 1002-1009.

239. Zhu, J., et al., *In situ stabilized carbon nanofiber (CNF) reinforced epoxy nanocomposites.* 2010. **20**(23): p. 4937-4948.

240. Abdalla, M., et al., *Cure behavior of epoxy/MWCNT nanocomposites: The effect of nanotube surface modification.* Polymer, 2008. **49**(15): p. 3310-3317.

241. Konnola, R. and K. Joseph, *Effect of side-wall functionalisation of multi-walled carbon nanotubes on the thermo-mechanical properties of epoxy composites.* RSC Advances, 2016. **6**(28): p. 23887-23899.

242. Park, Y.T., et al., *Epoxy Toughening with Low Graphene Loading.* Advanced Functional Materials, 2015. **25**(4): p. 575-585.

243. Tang, L.-c., et al., *Fracture mechanisms of epoxy filled with ozone functionalized multi-wall carbon nanotubes.* Composites Science and Technology, 2011. **72**(1): p. 7-13.

244. Ma, P.C., J.-K. Kim, and B.Z. Tang, *Effects of silane functionalization on the properties of carbon nanotube/epoxy nanocomposites.* Composites Science and Technology, 2007. **67**(14): p. 2965-2972.

245. Kim, M., et al., *Effect of surface treatment of graphene nanoplatelets for improvement of thermal and electrical properties of epoxy composites.* Carbon letters, 2015. **16**(1): p. 34-40.

246. Tseng, C.-H., C.-C. Wang, and C.-Y.J.C.o.M. Chen, *Functionalizing carbon nanotubes by plasma modification for the preparation of covalent-integrated epoxy composites.* 2007. **19**(2): p. 308-315.

247. Williams, J., et al., *Plasma treatment as a method for functionalising and improving dispersion of carbon nanotubes in epoxy resins.* Journal of Materials Science, 2012. **48**(3): p. 1005-1013.

248. Wan, Y.-J., et al., *Grafting of epoxy chains onto graphene oxide for epoxy composites with improved mechanical and thermal properties.* Carbon, 2014. **69**: p. 467-480.

249. Yao, H., S.A. Hawkins, and H.-J. Sue, *Preparation of epoxy nanocomposites containing well-dispersed graphene nanosheets.* Composites Science and Technology, 2017. **146**: p. 161-168.

250. Poutrel, Q.-A., et al., *Effect of pre and Post-Dispersion on Electro-Thermo-Mechanical Properties of a Graphene Enhanced Epoxy.* Applied Composite Materials, 2016. **24**(2): p. 313-336.

251. Tkalya, E.E., et al., *The use of surfactants for dispersing carbon nanotubes and graphene to make conductive nanocomposites.* Current Opinion in Colloid & Interface Science, 2012. **17**(4): p. 225-232.

252. Cha, J., et al., *Functionalization of carbon nanotubes for fabrication of CNT/epoxy nanocomposites.* Materials & Design, 2016. **95**: p. 1-8.

253. Loos, M.R., et al., *Effect of block-copolymer dispersants on properties of carbon nanotube/epoxy systems.* Composites Science and Technology, 2012. **72**(4): p. 482-488.

254. Geng, Y., et al., *Effects of surfactant treatment on mechanical and electrical properties of CNT/epoxy nanocomposites.* Composites Part A: Applied Science and Manufacturing, 2008. **39**(12): p. 1876-1883.

255. Wan, Y.-J., et al., *Improved dispersion and interface in the graphene/epoxy composites via a facile surfactant-assisted process.* Composites Science and Technology, 2013. **82**: p. 60-68.

256. Hameed, N., et al., *Individual dispersion of carbon nanotubes in epoxy via a novel dispersion-curing approach using ionic liquids.* Phys Chem Chem Phys, 2013. **15**(28): p. 11696-703.

257. Naeem, M., et al., *Epoxy/graphene nanocomposites prepared by in-situ microwaving.* Carbon, 2021. **177**: p. 271-281.

258. Zhang, H., E. Bilotti, and T. Peijs, *The use of carbon nanotubes for damage sensing and structural health monitoring in laminated composites: a review.* Nanocomposites, 2015. **1**(4): p. 167-184.

259. Rajak, D.K., et al., *Fiber-Reinforced Polymer Composites: Manufacturing, Properties, and Applications.* Polymers, 2019. **11**(10): p. 1667.

260. Ning, F., et al. *Additive manufacturing of CFRP composites using fused deposition modeling: effects of carbon fiber content and length*. in *ASME 2015 International Manufacturing Science and Engineering Conference*. 2015. American Society of Mechanical Engineers Digital Collection.

261. Koumoulos, E.P., et al., *Research and Development in Carbon Fibers and Advanced High-Performance Composites Supply Chain in Europe: A Roadmap for Challenges and the Industrial Uptake.* Journal of Composites Science, 2019. **3**(3): p. 86.

262. Mirabedini, A., et al., *Evolving Strategies for Producing Multiscale Graphene-Enhanced Fiber-Reinforced Polymer Composites for Smart Structural Applications.* 2020. **7**(11): p. 1903501.

263. Abdelal, N.R., M.H. Al-Saleh, and M.R. Irshidat, *Utilizing vacuum bagging process to prepare carbon fiber/CNT-modified-epoxy composites with improved mechanical properties.* Polymer-Plastics Technology and Engineering, 2018. **57**(3): p. 175-184.

264. Hsiao, K.-T., et al., *Effect of carbon nanofiber z-threads on mode-I delamination toughness of carbon fiber reinforced plastic laminates.* Composites Part A: Applied Science and Manufacturing, 2016. **91**: p. 324-335.

265. Kandare, E., et al., *Improving the through-thickness thermal and electrical conductivity of carbon fibre/epoxy laminates by exploiting synergy between graphene and silver nano-inclusions.* 2015. **69**: p. 72-82.

266. Santos, R.M., et al., *Multiscale carbon fibre–reinforced polymer (CFRP) composites containing carbon nanotubes with tailored interfaces.* Fatigue & Fracture of Engineering Materials & Structures, 2019. **42**(7): p. 1521-1533.

267. Godara, A., et al., *Influence of carbon nanotube reinforcement on the processing and the mechanical behaviour of carbon fiber/epoxy composites.* Carbon, 2009. **47**(12): p. 2914-2923.

268. Kostagiannakopoulou, C., et al., *On the interlaminar fracture toughness of carbon fiber composites enhanced with graphene nano-species.* 2015. **118**: p. 217-225.

269. Rodríguez-García, V., et al., *Industrial manufacturing and characterization of multiscale CFRP laminates made from prepregs containing graphene-related materials.* 2020. **7**(7): p. 075601.

270. Sánchez, M., et al., *Effect of the carbon nanotube functionalization on flexural properties of multiscale carbon fiber/epoxy composites manufactured by VARIM.* Composites Part B: Engineering, 2013. **45**(1): p. 1613-1619.

271. Zhou, Y., et al., *Improvement in mechanical properties of carbon fabric–epoxy composite using carbon nanofibers.* Journal of materials processing technology, 2008. **198**(1-3): p. 445-453.

272. Li, Y., et al., *Graphite nanoplatelet modified epoxy resin for carbon fibre reinforced plastics with enhanced properties.* Journal of Nanomaterials, 2017. **2017**.

273. Ramos-Fernandez, G., et al., *Role of graphene oxide surface chemistry on the improvement of the interlaminar mechanical properties of resin infusion processed epoxy-carbon fiber composites.* Polymer Composites, 2018. **39**(S4): p. E2116-E2124.

274. Li, Y., et al., *Graphene delivery systems for hierarchical fiber reinforced composites.* MRS Advances, 2016. **1**(19): p. 1339-1344.

275. Qin, W., et al., *Mechanical and electrical properties of carbon fiber composites with incorporation of graphene nanoplatelets at the fiber–matrix interphase.* 2015. **69**: p. 335-341.

276. Rodriguez, A.J., et al., *Mechanical properties of carbon nanofiber/fiber-reinforced hierarchical polymer composites manufactured with multiscale-reinforcement fabrics.* Carbon, 2011. **49**(3): p. 937-948.

277. Yuan, X., et al., *Influence of different surface treatments on the interfacial adhesion of graphene oxide/carbon fiber/epoxy composites.* Applied Surface Science, 2018. **458**: p. 996-1005.

278. Cheng, X., et al., *Improving the interlaminar shear strength and thermal conductivity of carbon fiber/epoxy laminates by utilizing the graphene-coated carbon fiber.* 2019. **136**(7): p. 47061.

279. Zhang, Z., et al., *The impact of carbon nanofibres on the interfacial properties of CFRPs produced with sized carbon fibres.* 2021. **13**(20): p. 3457.

280. Badakhsh, A., K.-H. An, and B.-J.J.P. Kim, *Enhanced Surface Energetics of CNT-Grafted Carbon Fibers for Superior Electrical and Mechanical Properties in CFRPs.* 2020. **12**(6): p. 1432.

281. Boroujeni, A., et al., *Hybrid carbon nanotube–carbon fiber composites with improved in-plane mechanical properties.* Composites Part B: Engineering, 2014. **66**: p. 475-483.

282. Islam, M.S., et al., *Grafting carbon nanotubes directly onto carbon fibers for superior mechanical stability: Towards next generation aerospace composites and energy storage applications.* 2016. **96**: p. 701-710.

283. Li, M., et al., *Interfacial improvement of carbon fiber/epoxy composites using a simple process for depositing commercially functionalized carbon nanotubes on the fibers.* 2013. **52**: p. 109-121.

284. Zhang, H., et al., *Improved fracture toughness and integrated damage sensing capability by spray coated CNTs on carbon fibre prepreg.* 2015. **70**: p. 102-110.

285. Breuer, O. and U. Sundararaj, *Big returns from small fibers: A review of polymer/carbon nanotube composites.* Polymer Composites, 2004. **25**(6): p. 630-645.

286. Sathyanarayana, S. and C. Hübner, *Thermoplastic Nanocomposites with Carbon Nanotubes*, in *Structural Nanocomposites*, J. Njuguna, Editor. 2013, Springer-Verlag: Berlin Heidelberg. p. 19-60.

287. De Volder, M.F.L., et al., *Carbon Nanotubes: Present and Future Commercial Applications.* Science, 2013. **339**(6119): p. 535-539.

288. Al-Saleh, M.H. and U. Sundararaj, *A review of vapor grown carbon nanofiber/polymer conductive composites.* Carbon, 2009. **47**(1): p. 2-22.

289. Mittal, G., et al., *A review on carbon nanotubes and graphene as fillers in reinforced polymer nanocomposites.* Journal of Industrial and Engineering Chemistry, 2015. **21**: p. 11-25.

290. Jang, B. and A. Zhamu, *Processing of nanographene platelets (NGPs) and NGP nanocomposites: a review.* Journal of Materials Science, 2008. **43**(15): p. 5092-5101.

291. Hänsch, S., et al., *Filler dispersion and electrical properties of polyamide 12/MWCNT-nanocomposites produced in reactive extrusion via anionic ring-opening polymerization.* Composites Science and Technology, 2012. **72**(14): p. 1671-1677.

292. Zhao, C.G., et al., *Synthesis and characterization of multi-walled carbon nanotubes reinforced polyamide 6 via in situ polymerization.* Polymer, 2005. **46**(14): p. 5125-5132.

293. Lu, K.B., et al., *Carbon Nanotube/Isotactic Polypropylene Composites Prepared by Latex Technology: Morphology Analysis of CNT-Induced Nucleation.* Macromolecules, 2008. **41**(21): p. 8081-8085.

294. Grunlan, J.C., et al., *Water-Based Single-Walled-Nanotube-Filled Polymer Composite with an Exceptionally Low Percolation Threshold.* Advanced Materials, 2004. **16**(2): p. 150-153.

295. Hufenus, R., et al., *Antistatic Fibers for High-Visibility Workwear: Challenges of Melt-Spinning Industrial Fibers.* Materials, 2020. **13**(11): p. 2645.

296. Bautista-Quijano, J.R., et al., *Strain sensing, electrical and mechanical properties of polycarbonate/multiwall carbon nanotube monofilament fibers fabricated by melt spinning.* Polymer, 2016. **82**: p. 181-189.

297. Kim, G.M., et al., *Relationships between phase morphology and deformation mechanisms in polymer nanocomposite nanofibres prepared by an electrospinning process.* Nanotechnology, 2006. **17**(4): p. 963-972.

298. Ameli, A., et al., *Electrical and dielectric properties of foam injection-molded polypropylene/multiwalled carbon nanotube composites.* AIP Conference Proceedings, 2015. **1664**: p. 110002.

299. Sun, Y.-C., et al., *Study on the thermoelectric properties of PVDF/MWCNT and PVDF/GNP composite foam.* Smart Materials and Structures, 2015. **24**(8): p. 085034.

300. Chen, L., R. Ozisik, and L.S. Schadler, *The influence of carbon nanotube aspect ratio on the foam morphology of MWNT/PMMA nanocomposite foams.* Polymer, 2010. **51**(11): p. 2368-2375.

301. Dorigato, A., et al., *Electrically conductive nanocomposites for fused deposition modelling.* Synthetic Metals, 2017. **226**: p. 7-14.

302. Hohimer, C.J., et al., *3D printed conductive thermoplastic polyurethane/carbon nanotube composites for capacitive and piezoresistive sensing in soft pneumatic actuators.* Additive Manufacturing, 2020. **34**: p. 101281.

303. Dai, Z., et al., *Creep-resistant behavior of MWCNT-polycarbonate melt spun nanocomposite fibers at elevated temperature.* Polymer, 2013. **54**: p. 3723-3729.

304. Ganß, M., et al., *Temperature Dependence of Creep Behavior of PP–MWNT Nanocomposites.* Macromolecular Rapid Communications, 2007. **28**: p. 1624-1633.

305. Pegel, S., et al., *Polymer-Carbon Nanotubes Composites: Melt Processing, Properties and Applications*, in *Synthetic Polymer-Polymer Composites*, D. Bhattacharyya and S. Fakirov, Editors. 2012, Carl Hanser Verlag: München. p. 145-192.

306. Grady, B.P., et al., *Nucleation of Polypropylene Crystallization by Single-Walled Carbon Nanotubes.* The Journal of Physical Chemistry B, 2002. **106**(23): p. 5852-5858.

307. Kashiwagi, T., et al., *Thermal and flammability properties of polypropylene/carbon nanotube nanocomposites.* Polymer, 2004. **45**(12): p. 4227-4239.

308. Schartel, B., et al., *Fire behaviour of polyamide 6/multiwall carbon nanotube nanocomposites.* European Polymer Journal, 2005. **41**(5): p. 1061-1070.

309. Boldt, R., et al., *Barrier Properties of GnP–PA-Extruded Films.* Polymers, 2020. **12**(3): p. 669.

310. Wolf, C., et al., *How the shape of fillers affects the barrier properties of polymer/non-porous particles nanocomposites: A review.* Journal of Membrane Science, 2018. **556**: p. 393-418.

311. Rybak, A., *Processing influence on thermal conductivity of polymer nanocomposites*, in *Processing of Polymer Nanocomposites*. 2019, Elsevier. p. 463-487.

312. Huang, C., X. Qian, and R. Yang, *Thermal conductivity of polymers and polymer nanocomposites.* Materials Science & Engineering R, 2018. **132**: p. 1-22.

313. Han, Z. and A. Fina, *Thermal conductivity of carbon nanotubes and their polymer nanocomposites: A review.* Progress in Polymer Science, 2011. **36**(7): p. 914-944.

314. Chen, J., et al., *Advances in Responsively Conductive Polymer Composites and Sensing Applications.* Polymer Reviews, 2021. **61**(1): p. 157-193.

315. Chung, D.D.L., *A critical review of piezoresistivity and its application in electrical-resistance-based strain sensing.* Journal of Materials Science, 2020. **55**(32): p. 15367-15396.

316. Obitayo, W. and T. Liu, *A Review: Carbon Nanotube-Based Piezoresistive Strain Sensors.* Journal of Sensors, 2012. **2012**: p. 652438.

317. Villmow, T., et al., *Polymer/carbon nanotube composites for liquid sensing: Model for electrical response characteristics.* Polymer, 2011. **52**: p. 2276-2285.

318. Li, Y., et al., *Electrical and vapor sensing behaviors of polycarbonate composites containing hybrid carbon fillers.* European Polymer Journal, 2018. **108**: p. 461-471.

319. Liu, Y., H. Zhang, and E. Bilotti, *Polymer Nanocomposites for Temperature Sensing and Self-regulating Heating Devices*, in *Polymer Nanocomposite Materials*. 2021. p. 247-266.

320. Sushmita, K., G. Madras, and S. Bose, *The journey of polycarbonate-based composites towards suppressing electromagnetic radiation.* Functional Composite Materials, 2021. **2**(1): p. 13.

321. Luo, J., et al., *Polypropylene-based melt mixed composites with singlewalled carbon nanotubes for thermoelectric applications: Switching from p-type to n-type by the addition of polyethylene glycol.* Polymer, 2017. **108**: p. 513-520.

322. Krause, B., et al., *Screening of different carbon nanotubes in melt-mixed polymer composites with different polymer matrices for their thermoelectric properties.* Journal of Composites Science, 2019. **3**(4): p. 106.

323. Krause, B., et al., *Characterization of dispersability of industrial nanotube materials and their length distribution before and after melt processing*, in *Carbon Nanotube-Polymer Composites*, D. Tasis, Editor. 2013, Royal Society of Chemistry: Cambridge, UK. p. 212-233.

324. Krause, B., et al., *Correlation of carbon nanotube dispersability in aqueous surfactant solutions and polymers.* Carbon, 2009. **47**(3): p. 602-612.

325. Müller, M., et al., *Effect of Graphite Nanoplate Morphology on the Dispersion and Physical Properties of Polycarbonate Based Composites.* Materials, 2017. **10**(5): p. 545.

326. Krause, B., et al., *Dispersability and particle size distribution of CNTs in an aqueous surfactant dispersion as a function of ultrasonic treatment time.* Carbon, 2010. **48**(10): p. 2746-2754.

327. Kasaliwal, G.R., et al., *Analysis of agglomerate dispersion mechanisms of multiwalled carbon nanotubes during melt mixing in polycarbonate.* Polymer, 2010. **51**(12): p. 2708-2720.

328. Kasaliwal, G.R., et al., *Influence of Material and Processing Parameters on Carbon Nanotube Dispersion in Polymer Melts*, in *Polymer-carbon Nanotube Composites: Preparation, Porperties and Applications*, T. McNally and P. Pötschke, Editors. 2011, Woodhead Publishing: Philadelphia, USA. p. 92-132.

329. Bhattacharyya, A.R., et al., *Styrene maleic anhydride copolymer mediated dispersion of single wall carbon nanotubes in polyamide 12: Crystallization Behavior and morphology.* Journal of Applied Polymer Science, 2007. **106**(1): p. 345-353.

330. Bhattacharyya, A.R., et al., *Reactive compatibilization of melt mixed PA6/SWNT composites: Mechanical properties and morphology.* Macromolecular Chemistry and Physics, 2005. **206**(20): p. 2084-2095.

331. Sathyanarayana, S., et al., *Influence of peroxide addition on the morphology and properties of polypropylene – multiwalled carbon nanotube nanocomposites.* Composites Science and Technology, 2013. **84**: p. 78-85.

332. Kasaliwal, G., A. Göldel, and P. Pötschke, *Influence of processing conditions in small-scale melt mixing and compression molding on the resistivity and morphology of polycarbonate–MWNT composites.* Journal of Applied Polymer Science, 2009. **112**(6): p. 3494-3509.

333. Villmow, T., et al., *Influence of twin-screw extrusion conditions on the dispersion of multi-walled carbon nanotubes in a poly(lactic acid) matrix.* Polymer, 2008. **49**(16): p. 3500-3509.

334. Al-Saleh, M.H. and U. Sundararaj, *Processing-microstructure-property relationship in conductive polymer nanocomposites.* Polymer, 2010. **51**(12): p. 2740-2747.

335. Mack, C., et al., *Twin-screw extrusion of multi walled carbon nanotubes reinforced polycarbonate composites: Investigation of electrical and mechanical properties.* IOP Conference Series: Materials Science and Engineering, 2012. **40**(1): p. 012020.

336. Villmow, T., B. Kretzschmar, and P. Pötschke, *Influence of screw configuration, residence time, and specific mechanical energy in twin-screw extrusion of polycaprolactone/multi-walled carbon nanotube composites.* Composites Science and Technology, 2010. **70**(14): p. 2045-2055.

337. Müller, M.T., et al., *Influence of feeding conditions in twin-screw extrusion of PP/MWCNT composites on electrical and mechanical properties.* Composites Science and Technology, 2011. **71**(13): p. 1535-1542.

338. Pötschke, P., et al., *Melt-Mixed PP/MWCNT Composites: Influence of CNT Incorporation Strategy and Matrix Viscosity on Filler Dispersion and Electrical Resistivity.* Polymers, 2019. **11**(2): p. 189.

339. Pötschke, P., T. Villmow, and B. Krause, *Melt mixed PCL/MWCNT composites prepared at different rotation speeds: Characterization of rheological, thermal, and electrical properties, molecular weight, MWCNT macrodispersion, and MWCNT length distribution.* Polymer, 2013. **54**(12): p. 3071-3078.

340. Piana, F. and J. Pionteck, *Effect of the melt processing conditions on the conductive paths formation in thermoplastic polyurethane/expanded graphite (TPU/EG) composites.* Composites Science and Technology, 2013. **80**: p. 39-46.

341. McClory, C., P. Pötschke, and T. McNally, *Influence of Screw Speed on Electrical and Rheological Percolation of Melt-Mixed High-Impact Polystyrene/MWCNT Nanocomposites.* Macromolecular Materials and Engineering, 2011. **296**(1): p. 59-69.

342. Santos, R.M., et al., *Effects of Particle Size and Surface Chemistry on the Dispersion of Graphite Nanoplates in Polypropylene Composites.* Polymers, 2018. **10**(2): p. 222.

343. He, S., et al., *Study on the morphology development and dispersion mechanism of polypropylene/graphene nanoplatelets composites for different shear field.* Composites Science and Technology, 2017. **153**(Supplement C): p. 209-221.

344. Rennhofer, H. and B. Zanghellini, *Dispersion State and Damage of Carbon Nanotubes and Carbon Nanofibers by Ultrasonic Dispersion: A Review.* Nanomaterials, 2021. **11**(6): p. 1469.

345. Gao, X., A.I. Isayev, and C. Yi, *Ultrasonic treatment of polycarbonate/carbon nanotubes composites.* Polymer, 2016. **84**: p. 209-222.

346. Zhong, J., A.I. Isayev, and K. Huang, *Influence of ultrasonic treatment in PP/CNT composites using masterbatch dilution method.* Polymer, 2014. **55**(7): p. 1745-1755.

347. Isayev, A.I., R. Kumar, and T.M. Lewis, *Ultrasound assisted twin screw extrusion of polymer-nanocomposites containing carbon nanotubes.* Polymer, 2009. **50**(1): p. 250-260.

348. Krause, B., J. Carval, and P. Pötschke, *Influence of mixing conditions on carbon nanotube shortening and curling in polycarbonate composites.* AIP Conference Proceedings, 2017. **1914**(1): p. 030007.

349. Liebscher, M., et al., *Electrical and melt rheological characterization of PC and co-continuous PC/SAN blends filled with CNTs: Relationship between melt-mixing parameters, filler dispersion, and filler aspect ratio.* Journal of Polymer Science Part B: Polymer Physics, 2018. **56**(1): p. 79-88.

350. Müller, M.T., P. Pötschke, and B. Voit, *Dispersion of carbon nanotubes into polyethylene by an additive assisted one-step melt mixing approach.* Polymer, 2015. **66**: p. 210-221.

351. Socher, R., B. Krause, and P. Pötschke, *Effect of additives on MWCNT dispersion and electrical percolation in polyamide 12 composites.* AIP Conference Proceedings, 2017. **1914**(1): p. 030016.

352. Socher, R., et al., *Interfacial chemistry using a bifunctional coupling agent for enhanced electrical properties of carbon nanotube based composites.* Polymer, 2013. **54**(20): p. 5391-5398.

353. Chen, J., et al., *Interfacial characteristics of carbon nanotube-polymer composites: A review.* Composites Part A: Applied Science Manufacturing, 2018. **114**: p. 149-169.

354. Kasgoz, A., et al., *Effect of different types of carbon fillers on mechanical and rheological properties of cyclic olefin copolymer (COC) composites.* Composites Part B: Engineering, 2014. **66**: p. 126-135.

355. Verma, R., M. Rathod, and R. Goyal. *A review on the effect of processing techniques and functionalization of filler on mechanical properties of polymer nanocomposites*. in *IOP Conference Series: Materials Science and Engineering*. 2020. IOP Publishing.

356. Chaudhry, F.N., et al., *Effect of carbon fibre on reinforcement of thermoplastics using FDM and RSM.* Journal of Thermoplastic Composite Materials, 2022. **35**(3): p. 352-374.

357. Mohd Radzuan, N.A., et al., *Electrical conductivity performance of predicted modified fibre contact model for multi-filler polymer composite.* Polymers, 2019. **11**(9): p. 1425.

358. López-González, M., et al., *Graphene and polyethylene: A strong combination towards multifunctional nanocomposites.* Polymers, 2020. **12**(9): p. 2094.

359. Alateyah, A., *High-Density Polyethylene Based on Exfoliated Graphite Nanoplatelets/Nano-Magnesium Oxide: An Investigation of Thermal Properties and Morphology.* Materials Sciences Applications, 2019. **10**(03): p. 159.

360. Zhou, Z., et al., *Effect of different carbon fillers on the properties of PP composites: comparison of carbon black with multiwalled carbon nanotubes.* Journal of Applied Polymer Science, 2006. **102**(5): p. 4823-4830.

361. Wang, R., et al., *Fabrication of high mechanical performance UHMWPE nanocomposites with high-loading multiwalled carbon nanotubes.* Journal of Applied Polymer Science, 2020. **137**(19): p. 48667.

362. Nisar, M., et al., *Polyethylene Nanocomposites with Ni, Co, and Fe Carbon-Based Magnetic Fillers.* Polymer Engineering Science, 2020. **60**(5): p. 988-995.

363. Dal Lago, E., et al., *Influence of different carbon-based fillers on electrical and mechanical properties of a PC/ABS blend.* Polymers, 2019. **12**(1): p. 29.

364. Myalski, J., M. Godzierz, and P. Olesik, *Effect of carbon fillers on the wear resistance of pa6 thermoplastic composites.* Polymers, 2020. **12**(10): p. 2264.

365. Kasgoz, A., D. Akın, and A. Durmus, *Rheological and electrical properties of carbon black and carbon fiber filled cyclic olefin copolymer composites.* Composites Part B: Engineering, 2014. **62**: p. 113-120.

366. Qiu, F., X. Yin, and J.P. Qu, *Formation of polypropylene/functional graphene oxide nanocomposites with Different FGs loading in elongation flow condition.* Polymer Engineering Science, 2019. **59**(4): p. 830-837.

367. Shanmugam, L., et al., *Enhanced interphase between thermoplastic matrix and UHMWPE fiber sized with CNT-modified polydopamine coating.* 2019. **174**: p. 212-220.

368. Vilaverde, C., et al., *Dispersion and re-agglomeration of graphite nanoplates in polypropylene melts under controlled flow conditions.* Composites Part A: Applied Science Manufacturing, 2015. **78**: p. 143-151.

369. Kamarudin, S.H., et al., *Mechanical and physical properties of Kenaf-reinforced Poly (lactic acid) plasticized with epoxidized Jatropha Oil.* 2019. **14**(4): p. 9001-9020.

370. Chandrasekar, M., et al., *Inorganic Nanofillers-Based Thermoplastic and Thermosetting Composites*, in *Lightweight Polymer Composite Structures*. 2020, CRC Press. p. 309-330.

371. Nurazzi, N., et al., *Mechanical Performance and Applications of CNTs Reinforced Polymer Composites—A Review.* 2021. **11**(9): p. 2186.

372. Samuel, J., et al., *Effect of carbon nanotube (CNT) loading on the thermomechanical properties and the machinability of CNT-reinforced polymer composites.* 2009. **131**(3).

373. ÖZTÜRK, E., et al., *Optimization of hybrid thermoplastic composite production via artificial intelligent approach*, in *Automotive Composites Conference & Exhibition*. 2021: Michigan, USA.

374. Batten, S.R., et al., *Coordination polymers, metal–organic frameworks and the need for terminology guidelines.* CrystEngComm, 2012. **14**(9): p. 3001-3004.

375. Raptopoulou, C.P., *Metal-organic frameworks: Synthetic methods and potential applications.* Materials 2021. **14**(2): p. 310.

376. Andirova, D., et al., *Effect of the structural constituents of metal organic frameworks on carbon dioxide capture.* Microporous Mesoporous Materials, 2016. **219**: p. 276-305.

377. Wang, H.-S., *Metal–organic frameworks for biosensing and bioimaging applications.* Coordination Chemistry Reviews, 2017. **349**: p. 139-155.

378. Mallakpour, S., E. Nikkhoo, and C.M. Hussain, *Application of MOF materials as drug delivery systems for cancer therapy and dermal treatment.* Coordination Chemistry Reviews, 2022. **451**: p. 214262.

379. Xu, B., et al., *Recent progress in metal-organic framework-based supercapacitor electrode materials.* Coordination Chemistry Reviews, 2020. **420**: p. 213438.

380. Hu, M.-L., et al., *Sensing organic analytes by metal–organic frameworks: a new way of considering the topic.* Inorganic Chemistry Frontiers, 2020. **7**(7): p. 1598-1632.

381. Li, S. and F. Huo, *Metal–organic framework composites: from fundamentals to applications.* Nanoscale 2015. **7**(17): p. 7482-7501.

382. Yusuf, K., A. Aqel, and Z. ALOthman, *Metal-organic frameworks in chromatography.* Journal of Chromatography A, 2014. **1348**: p. 1-16.

383. Jiao, L., et al., *Metal–organic frameworks: Structures and functional applications.* Materials Today 2019. **27**: p. 43-68.

384. Huang, B., Y. Li, and W. Zeng, *Application of Metal-Organic Framework-Based Composites for Gas Sensing and Effects of Synthesis Strategies on Gas-Sensitive Performance.* Chemosensors, 2021. **9**(8): p. 226.

385. Bhardwaj, S.K., et al., *An overview of different strategies to introduce conductivity in metal–organic frameworks and miscellaneous applications thereof.* Journal of Materials Chemistry A, 2018. **6**(31): p. 14992-15009.

386. Lei, J., et al., *Design and sensing applications of metal–organic framework composites.* TrAC Trends in Analytical Chemistry, 2014. **58**: p. 71-78.

387. Sosa, J.D., et al., *Metal–organic framework hybrid materials and their applications.* Crystals, 2018. **8**(8): p. 325.

388. Chen, L., et al., *The function of metal–organic frameworks in the application of MOF-based composites.* Nanoscale Advances, 2020. **2**(7): p. 2628-2647.

389. Kalaj, M., et al., *MOF-polymer hybrid materials: From simple composites to tailored architectures.* Chemical reviews, 2020. **120**(16): p. 8267-8302.

390. Wang, X., Y. Wang, and Y. Ying, *Recent advances in sensing applications of metal nanoparticle/metal–organic framework composites.* Trends in Analytical Chemistry, 2021. **143**: p. 116395.

391. Chronopoulos, D.D., et al., *Carbon Nanotube Based Metal–Organic Framework Hybrids From Fundamentals Toward Applications.* Small, 2022. **18**(4): p. 2104628.

392. Meng, H., et al., *Changing the hydrophobic MOF pores through encapsulating fullerene C60 and metallofullerene Sc3C2@ C80.* The Journal of Physical Chemistry C, 2019. **123**(10): p. 6265-6269.

393. Ko, M., et al., *Drawing sensors with ball-milled blends of metal-organic frameworks and graphite.* Sensors 2017. **17**(10): p. 2192.

394. Petit, C., J. Burress, and T.J. Bandosz, *The synthesis and characterization of copper-based metal–organic framework/graphite oxide composites.* Carbon, 2011. **49**(2): p. 563-572.

395. Liu, X.-W., et al., *Composites of metal–organic frameworks and carbon-based materials: preparations, functionalities and applications.* Journal of Materials Chemistry A, 2016. **4**(10): p. 3584-3616.

396. Jahan, M., et al., *Structure-directing role of graphene in the synthesis of metal− organic framework nanowire.* Journal of the American Chemical Society, 2010. **132**(41): p. 14487-14495.

397. Vaitsis, C., G. Sourkouni, and C. Argirusis, *Sonochemical synthesis of MOFs*, in *Metal-Organic Frameworks for Biomedical Applications*. 2020, Elsevier. p. 223-244.

398. Klinowski, J., et al., *Microwave-assisted synthesis of metal–organic frameworks.* Dalton Transactions, 2011. **40**(2): p. 321-330.

399. Bian, Z., et al., *Interfacial growth of metal organic framework/graphite oxide composites through pickering emulsion and their CO2 capture performance in the presence of humidity.* Langmuir, 2015. **31**(26): p. 7410-7417.

400. Szczęśniak, B., J. Choma, and M. Jaroniec, *Ultrahigh benzene adsorption capacity of graphene-MOF composite fabricated via MOF crystallization in 3D mesoporous graphene.* Microporous Mesoporous Materials, 2019. **279**: p. 387-394.

401. Stiff-Roberts, A.D. and W. Ge, *Organic/hybrid thin films deposited by matrix-assisted pulsed laser evaporation (MAPLE).* Applied Physics Reviews, 2017. **4**(4): p. 041303.

402. Chrisey, D.B., et al., *Laser deposition of polymer and biomaterial films.* Chemical Reviews, 2003. **103**(2): p. 553-576.

403. M. Alfè, V.G., G. Minopoli, U. Caruso, G. Ausanio, *Thin coating through Matrix-Assisted Pulsed Laser Evaporation with new-concept biocompatible graphenic materials.* 2022.

404. Ausanio, G., et al., *Laser deposition from a lava stone cup.* Optics Laser Technology, 2020. **131**: p. 106432.

405. Ausanio, G., et al., *Matrix-assisted pulsed laser evaporation of β-glucosidase from a dopa/quinone target.* Enzyme Microbial Technology, 2020. **132**: p. 109414.

406. Bloisi, F., et al., *Biomaterial thin film deposition and characterization by means of MAPLE technique.* Materials Science Engineering: C, 2007. **27**(5-8): p. 1185-1190.

407. Paun, I.A., et al., *Thin films of polymer blends for controlled drug delivery deposited by matrix-assisted pulsed laser evaporation.* Applied Physics Letters, 2010. **96**(24): p. 243702.

408. Bloisi, F., et al., *Effect of substrate temperature on MAPLE deposition of synthetic eumelanin films.* Applied Physics A, 2011. **105**(3): p. 619-627.

409. Piqué, A., et al., *Use of Matrix Assisted Pulsed Laser Evaporation (Maple) for the growth of organic thin films.* MRS Online Proceedings Library, 1998. **526**.

410. Califano, V., et al., *Frozen microemulsions for MAPLE immobilization of lipase.* Molecules, 2017. **22**(12): p. 2153.

411. Martino, M., et al., *Pulsed laser deposition of organic and biological materials.* Journal of Materials Science: Materials in Electronics, 2009. **20**(1): p. 435-440.

412. Marturano, V., et al., *Smart coatings prepared via MAPLE deposition of polymer nanocapsules for light-induced release.* Molecules, 2021. **26**(9): p. 2736.

413. Piqué, A., *The matrix-assisted pulsed laser evaporation (MAPLE) process: origins and future directions.* Applied Physics A, 2011. **105**(3): p. 517-528.